

Validation of Vehicle Model in Car Simulator

C H R I S T I N A W E S T E R M A R K

Master of Science Thesis
Stockholm, Sweden 2013

Validation of Vehicle Model in Car Simulator

C H R I S T I N A W E S T E R M A R K

Master's Thesis in Aerospace Engineering (30 ECTS credits)
Master Programme in Systems Engineering (120 credits)
Royal Institute of Technology year 2013
Supervisor at KTH was Per Enqvist
Examiner was Per Engvist

TRITA-MAT-E 2013:042
ISRN-KTH/MAT/E--13/042--SE

Royal Institute of Technology
School of Engineering Sciences

KTH SCI
SE-100 44 Stockholm, Sweden

URL: www.kth.se/sci

Abstract

The vehicle model validated in this thesis is developed by BorgWarner TTS to be used for control algorithm design. The validation process included measurements on the car in both winter and summer conditions. The model is simulated with Matlab Simulink and the measurement data is used as input to the model and also for comparison between result and simulated output. This was done as a master thesis at Kungliga Tekniska Högskolan in Stockholm.

Contents

1	Introduction	4
1.1	Background	4
1.2	Problem formulation	4
1.3	Approach	4
1.4	Related work	4
2	Vehsim simulation environment overview	6
2.1	Vehicle model	6
2.1.1	Chassis	6
2.1.2	Tire	7
2.1.3	Power train	7
2.1.4	Fuel consumption	7
3	Theory of Bicycle Model	8
3.1	Rotating coordinate systems	8
3.2	Model overview	8
3.3	Equations of motion, bicycle model	9
3.4	Tires in bicycle model	10
4	Vehicle model in Vehsim	12
4.1	Coordinate systems	12
4.1.1	Body fixed and global coordinate systems	12
4.1.2	Wheel coordinate system	12
4.1.3	Transformation between coordinate systems using Euler Angles	13
4.2	Chassis	15
4.2.1	Translational equations of motion	15
4.2.2	Rotational equations of motion	15
4.2.3	Suspension	17
4.2.4	Anti-roll bar	18
4.2.5	Steering kinematics	19
4.3	Tires in Vehsim vehicle model	20
4.3.1	Pure Slip	20
4.3.2	Combined Slip	20

5 Measurements	21
5.1 Test car data	21
5.2 Test maneuvers	22
5.2.1 Offset Run	22
5.2.2 Step with gear in neutral position	22
5.2.3 Step in steer angle	22
5.2.4 Sinus driving	22
5.2.5 Handling tracks	22
5.3 Measurement equipment	23
5.3.1 Accelerometer	23
5.3.2 Optical velocity sensor	23
6 Simulation	24
6.1 Signals	24
6.1.1 Filtering of measurement signals	24
6.1.2 Accelerations	24
6.1.3 Velocities	25
6.1.4 Wheel rotation and wheel speed	25
6.1.5 Yaw Rate and and Yaw Acceleration	25
6.1.6 Steering Angle	26
6.2 Simulation of bicycle model	26
6.3 Simulation of Vehsim vehicle model for optimization of parameters	27
7 Optimization and validation	29
7.1 Theory of optimization part	29
7.1.1 Error	29
7.2 Preparation of measurement files for optimization	30
7.2.1 Offset calculations	30
7.2.2 Add measurement files	30
7.2.3 Optimization index	30
7.2.4 Steady state index for tire optimization	30
7.2.5 Scaling	31
7.3 Bicycle model parameters optimization	31
7.4 Optimization of Vehsim vehicle model parameters	32
7.4.1 Wheel radius optimization	32
7.4.2 Tire parameters optimization	32
7.4.3 Chassis parameters optimization	33
7.5 Validation	33
8 Results	34
8.1 Result of bicycle model optimization	34
8.2 Result of wheel radius optimization for Vehsim vehicle model	36
8.3 Result of Vehsim vehicle model tire parameters optimization	37
8.4 Optimization of chassis parameters	38

8.4.1	Static Camber Angle and Bump Steer	38
8.4.2	Static Camber Angle, Bump Steer and Static Toe Angle	40
8.4.3	Static Camber Angle, Bump Steer, Static Toe Angle and Camber Suspension Ratio	42
8.4.4	Static Camber Angle, Bump Steer, Static Toe Angle, Camber Suspension Ratio and Camber Steer Ratio	44
9	Discussion	47
9.1	Scaling	47
9.2	Error	47
9.3	Choice of chassis parameters	47
9.4	Result of bicycle model optimization	48
9.5	Result of Vehsim vehicle model optimization	48
9.5.1	Radius optimization	48
9.5.2	Tire optimization	48
9.5.3	Chassis parameters, high road friction	49
9.5.4	Chassis parameters, low road friction	49
9.6	Comparison between bicycle model and Vehsim vehicle model	49
9.7	Optimization method	49
10	Conclusions	50
10.1	Vehsim vehicle model	50
10.2	Bicycle model	50
A	Nomenclature	53
B	Vehsim signals	56
B.1	Chassis	56
B.2	Tire	57
B.3	Power train	57
B.4	Fuel consumption	57
B.5	Driver	58
B.6	Road	58

1 | Introduction

1.1 Background

BorgWarner TTS in Landskrona has developed a simulation environment in Matlab Simulink called Vehsim that is built to be used for development and test of control software. The usage of the simulation environment requires a validated vehicle model and the scope of this master thesis is to validate the model using measurement data from driving maneuvers in low- and high friction conditions.

1.2 Problem formulation

The vehicle model in Vehsim is based on different physical expressions and there are several parameters in the model that can be varied to change the behavior of the simulated car. Examples of parameters are road friction, tire stiffness and steering characteristics as toe and camber angles. The problem in this master thesis is to identify important parameters in the vehicle model and use measured data from testings in a real car to fit the parameters and in that way make the behavior of the simulated vehicle as close to a real car as possible.

1.3 Approach

The work of fit parameters to measurement data to validate the model was done for two models with different complexity. The first, more simple one is a bicycle model and the second is the vehicle model used in Vehsim. The models were simulated in Matlab Simulink and the data used were measured in a Volkswagen Golf. Measurement signals from the driving maneuvers is used in the Simulink models both as inputs and for comparison between simulated and measured data. The identified parameters were optimized for the two models and the result is presented in the report.

1.4 Related work

The master thesis *Estimation of Vehicle Lateral Velocity* by Pierre Pettersson, Haldex Traction AB, 2008 was used to get understanding for the vehicle model, [10].

There are many articles that treat the subject of identifying vehicle parameters, for example *Car*

Parameters Identification by Handling Manoeuvres by Michele Russo, Riccardo Russo and Agsotino Volpe, [11] and also *Modeling, Simulation and Validation of 14 DOF Full Vehicle Model* by Joga Dharma Setiawan, Mochamad Safarudin and Amrik Singh, [12].

2 | Vehsim simulation environment overview

Vehsim is a car simulation environment built in Matlab Simulink and this chapter will give an overview of how it is structured and the signals that are used in the built in vehicle model in Vehsim. The Vehsim Simulink model, that can be seen in *Figure 2.1*, consists of the modules *Vehicle*, *Driver*, *Road* and *Control Software*. Tables with names of all inputs and outputs can be found in *Appendix B*

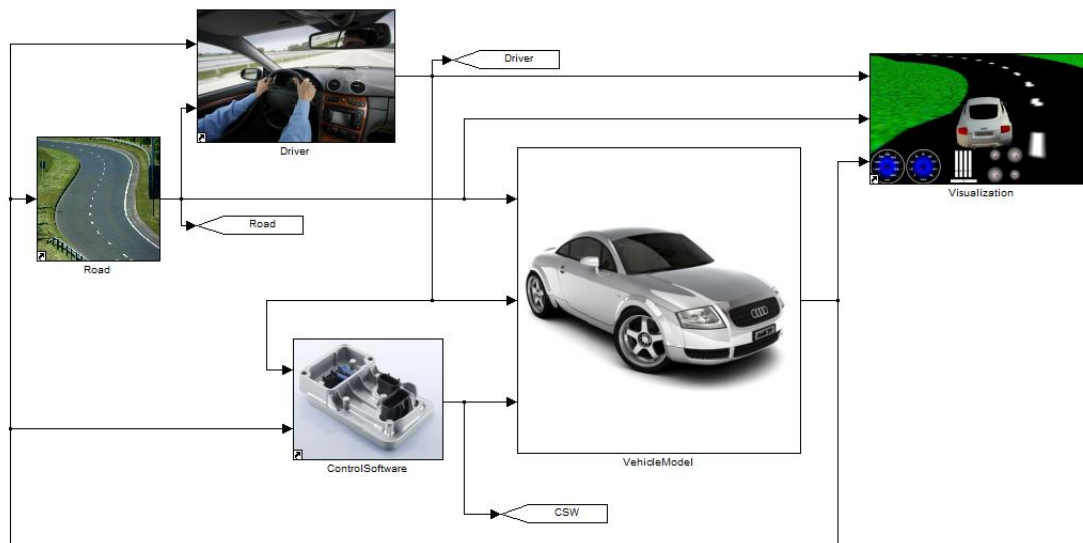


Figure 2.1: An overview of the top layer in the simulation environment Vehsim containing the blocks Vehicle, control software, driver, road and visualization

2.1 Vehicle model

The vehicle model block in Vehsim is built of *Chassis*, *Power train*, *Tire* and *Fuel consumption* blocks see *Figure 2.2* for an overview of the vehicle model.

2.1.1 Chassis

The input signals to the chassis model are steering wheel angle from the driver block and tire forces from the tire block. Example of outputs are positions and velocities of the vehicle body and the

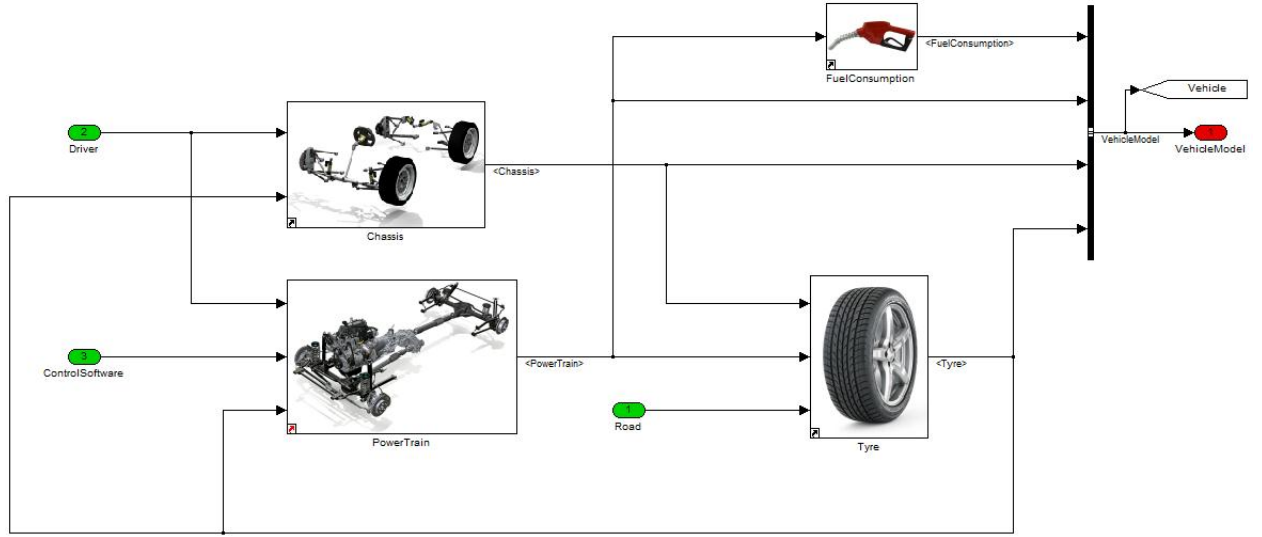


Figure 2.2: An overview of the vehicle model in Vehsim containing the blocks chassis, power train, tire and fuel consumption

wheel hubs. Other output signals are accelerations and roll-, pitch- and yaw rate. The chassis model also calculates transformation matrices between the different coordinate systems that are needed to describe the motion of the vehicle.

2.1.2 Tire

Inputs to the tire model comes from the blocks chassis, road and power train. Example of inputs are hub velocity from the chassis block, road normal and friction from the road block and drive shaft torque and brake torque from the power train block. The tire model calculates the forces that develops by the tires, the rotational speed of the wheels and tire torques.

2.1.3 Power train

The power train model uses information from the driver block about the status of for example the brake, clutch, gear and throttle pedals. Input from the tire block is wheel rotational speed and the power train also gets signals from the control software. Outputs of the model are hub torque, hub brake torque, engine rotational speed and engine torque.

2.1.4 Fuel consumption

The fuel consumption model uses information about the engine rotational speed and engine torque to calculate fuel consumption rate and consumed fuel.

3 | Theory of Bicycle Model

A simple but still informative model of the motion of a vehicle is the so called bicycle model. This chapter handles the theory needed to derive the equations of motion for the bicycle model that are simulated in *Chapter 6*. The theory in this chapter comes from [7].

3.1 Rotating coordinate systems

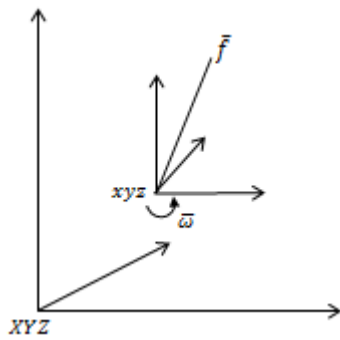


Figure 3.1: Rotating Coordinate system

The equations of motion are derived using Newton's second law and the accelerations of the vehicle must therefore be expressed in an inertial system. The derivation of a vector \bar{f} located in the local coordinate system xyz that is rotated $\bar{\omega}$ relative to the inertial system XYZ is given by

$$\frac{d\bar{f}}{dt} = \frac{\partial \bar{f}}{\partial t} + \bar{\omega} \cdot \bar{f} \quad (3.1)$$

where $\frac{\partial \bar{f}}{\partial t}$ is the derivative of the vector \bar{f} in the rotating coordinate system.

3.2 Model overview

Figure 3.2 shows the bicycle model with coordinate systems and forces. The front wheel is steered by changing the angle δ . The center of gravity is located a distance l_f from the front wheel and l_r from the rear wheel. The forces acting on the vehicle are the tires forces F_{12} and F_{34} . Two coordinate

systems are needed to describe the motion of the vehicle, the xy system is fixed in the center of gravity of the vehicle body and the XY system is a global landscape fixed system.

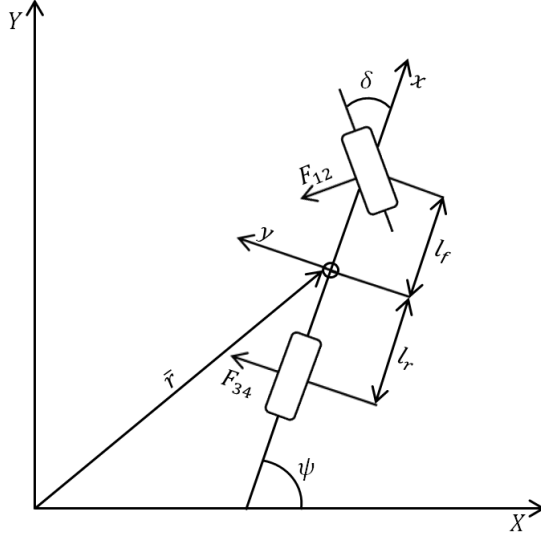


Figure 3.2: Bicycle model

3.3 Equations of motion, bicycle model

The translational equations of motion for the bicycle model are derived from Newton's second law

$$\sum F = m \cdot \bar{a} \quad (3.2)$$

where $\sum F$ is the sum of the forces that acts on the center of gravity, m is the mass of the vehicle and \bar{a} is the acceleration of the center of gravity.

The rotational equation for planar motion is given by

$$\sum M = I_{zz} \ddot{\psi} \quad (3.3)$$

where $\sum M$ is the sum of the moments around the center of gravity, I_{zz} is the moment of inertia around the z-axis and $\ddot{\psi}$ is the angular acceleration of the yaw angle ψ .

The acceleration of the center of gravity, \bar{a} is the second derivative of \bar{r} , which is the position vector from the origin of global coordinate system to the center of gravity of the vehicle, see Figure 3.2. The velocity of the center of gravity expressed in the global system is

$$\dot{\bar{r}} = v_x \cdot \hat{e}_x + v_y \cdot \hat{e}_y \quad (3.4)$$

where v_x and v_y are the velocity in x - and y -direction and \hat{e}_x and \hat{e}_y are the x and y components of a unit vector. The acceleration of the center of gravity is the derivative of equation (3.4) as per

equation (3.1) with $\bar{\omega} = \dot{\psi} \cdot \hat{e}_z$ and $\bar{f} = \dot{r}$.

$$\ddot{r} = (\dot{v}_x - \dot{\psi} v_y) \cdot \hat{e}_x + (\dot{v}_y + \dot{\psi} v_x) \cdot \hat{e}_y \quad (3.5)$$

It is assumed that the only forces acting on the vehicle body are the tire forces F_{12} and F_{34} . By summing the forces acting on the center of gravity and using equation (3.2) and (3.5) the lateral equation of motion is derived as

$$m(\dot{v}_y + \dot{\psi} v_x) = F_{34} + F_{12} \cos \delta \quad (3.6)$$

The rotational equation of motion are given by summing the moments around center of gravity together with equation (3.3)

$$I_z \ddot{\psi} = l_f F_{12} \cos \delta - l_r F_{34} \quad (3.7)$$

3.4 Tires in bicycle model

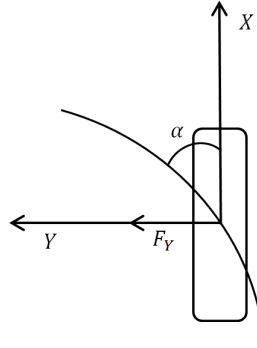


Figure 3.3: Tire model in Simulink

The tire forces F_{12} and F_{34} are assumed to be linear functions of the drift angles α_{12} and α_{34} . The side forces on the front and rear tires are described by:

$$\begin{aligned} F_{12} &= -C_{12} \cdot \alpha_{12} \\ F_{34} &= -C_{34} \cdot \alpha_{34} \end{aligned} \quad (3.8)$$

where C_{12} and C_{34} are tire coefficient. The drift angles α_{12} and α_{34} are the angle between longitudinal and lateral velocities. The velocities of front and rear wheels are

$$\dot{r}_f = \dot{r} + \bar{\omega} \times (l_f, 0, 0) = v_x \cdot \hat{e}_x + (v_y + \dot{\psi} l_f) \cdot \hat{e}_y \quad (3.9)$$

$$\dot{r}_r = \dot{r} + \bar{\omega} \times (-l_r, 0, 0) = v_x \cdot \hat{e}_x + (v_y - \dot{\psi} l_r) \cdot \hat{e}_y \quad (3.10)$$

When calculating the drift angle on the front wheel the steering angle δ also needs to be considered. The drift angles are

$$\begin{aligned} \alpha_{12} &= \arctan\left(\frac{v_y + \dot{\psi} l_f}{v_x}\right) - \delta \\ \alpha_{34} &= \arctan\left(\frac{v_y - \dot{\psi} l_r}{v_x}\right) \end{aligned} \quad (3.11)$$

The equations of motion for the bicycle model are given by equation (3.6) and (3.7) together with equation (3.8) and (3.11).

4 | Vehicle model in Vehsim

The vehicle model in Vehsim is a four wheel car that consists of *chassis*-, *power train*- and *tire* modules. The model used to optimize parameters is a bit simplified compare to the complete vehicle model in Vehsim, that is because some calculations are replaced by measurement data inserted in the simulation. The *power train* module is replaced with data of wheel speed. The two remaining modules in the vehicle module, *chassis* and *tire* are described below.

4.1 Coordinate systems

The coordinate systems needed to describe the motion of the vehicle are a global system, a body fixed system and one system fixed in each of the wheel hubs.

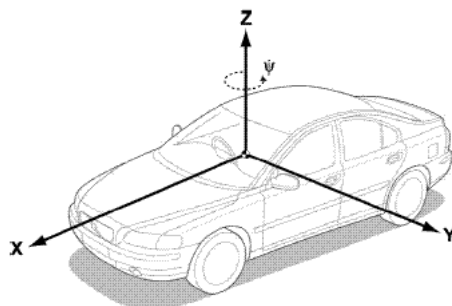


Figure 4.1: Vehicle body coordinate system that follows the ISO-standard

4.1.1 Body fixed and global coordinate systems

The body fixed coordinate system has its origin in the center of gravity of the vehicle and travels with it. The coordinate system follows the ISO-standard meaning that the X-axis is positive forward, the Y-axis is positive to the left and the Z-axis is positive upwards, see *Figure 4.1*. The global coordinate system is fixed to earth and the body fixed system is rotating in the global system. [9]

4.1.2 Wheel coordinate system

Figure 4.2 shows two different coordinate systems, the C-axis and the W-axis system. The C-axis system has its origin in the wheel center and is fixed to the wheel carrier while the W-axis has its

origin in the contact point between wheel and road. Inputs and output to the tire model are given in the C-axis system, the tire model transforms the information to the W-axis system before making calculations. [6]

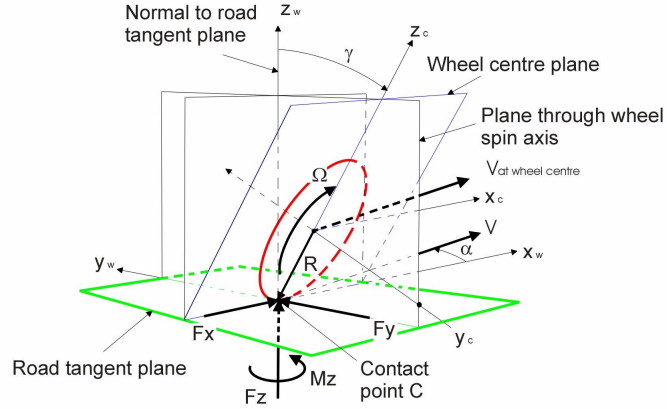


Figure 4.2: Wheel coordinate system

4.1.3 Transformation between coordinate systems using Euler Angles

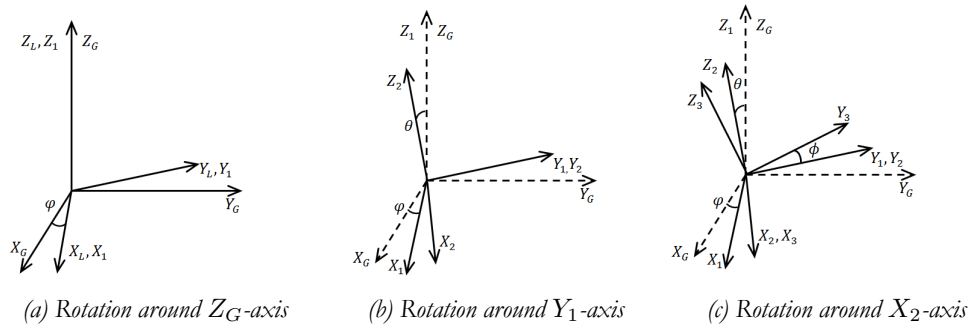


Figure 4.3: Rotation of coordinate system described by Euler Angles

The use of different coordinate systems in the same model requires that transformations of forces and velocities between the systems must take place. The rotation of a body fixed local system in a global coordinate system can be described by the Euler angles. The angles are

ϕ	Roll - rotation around X-axis
θ	Pitch - rotation around Y-axis
ψ	Yaw - rotation around Z-axis

The orientation of the local coordinate system in the global coordinate system is described by making rotations of the local system in a certain order, resulting in a transformation matrix between the

two coordinate systems. There are different conventions for the order of rotation and the resulting transformation matrix is dependent of the order in which the rotations are carried out, in this case the z-y-x convention is used.

The global $X_G Y_G Z_G$ and the local $X_L Y_L Z_L$ coordinate systems are superimposed to start with and the first step is to rotate the local coordinate system an angle ψ around the common Z-axis, see *Figure 4.3a*. In this orientation a new coordinate system $X_1 Y_1 Z_1$ is denoted, where the Z_G and Z_1 axes are aligned. A unit vector with components $(\hat{e}_x, \hat{e}_y, \hat{e}_z)$ in the global $X_G Y_G Z_G$ coordinate system can be expressed as components $(\hat{e}_{x1}, \hat{e}_{y1}, \hat{e}_{z1})$ in the new $X_1 Y_1 Z_1$ with the equations

$$\begin{aligned}\hat{e}_{x1} &= \hat{e}_x \cos(\psi) + \hat{e}_y \sin(\psi) \\ \hat{e}_{y1} &= -\hat{e}_x \sin(\psi) + \hat{e}_y \cos(\psi) \\ \hat{e}_{z1} &= \hat{e}_z\end{aligned}\tag{4.1}$$

The second step is to rotate the $X_1 Y_1 Z_1$ system around the Y_1 axis an angle θ and denote a new coordinate system $X_2 Y_2 Z_2$, see *Figure 4.3b*. Transformation of a unit vector $(\hat{e}_{x1}, \hat{e}_{y1}, \hat{e}_{z1})$ to components $(\hat{e}_{x2}, \hat{e}_{y2}, \hat{e}_{z2})$ in the $X_2 Y_2 Z_2$ system are given by

$$\begin{aligned}\hat{e}_{x2} &= \hat{e}_{x1} \cos(\theta) - \hat{e}_{z1} \sin(\theta) \\ \hat{e}_{y2} &= \hat{e}_{y1} \\ \hat{e}_{z2} &= \hat{e}_{x1} \sin(\theta) + \hat{e}_{z1} \cos(\theta)\end{aligned}\tag{4.2}$$

The last step is to rotate $X_2 Y_2 Z_2$ around the X_2 axis an angle ϕ and denote a new coordinate system $X_3 Y_3 Z_3$ where X_2 and X_3 are aligned, see *Figure 4.3c*. Components $(\hat{e}_{x2}, \hat{e}_{y2}, \hat{e}_{z2})$ of a vector in the $X_2 Y_2 Z_2$ system can be expressed as $(\hat{e}_{x3}, \hat{e}_{y3}, \hat{e}_{z3})$ in the $X_3 Y_3 Z_3$ system with equations

$$\begin{aligned}\hat{e}_{x3} &= \hat{e}_{x2} \\ \hat{e}_{y3} &= \hat{e}_{y2} \cos(\phi) + \hat{e}_{z2} \sin(\phi) \\ \hat{e}_{z3} &= -\hat{e}_{y2} \sin(\phi) + \hat{e}_{z2} \cos(\phi)\end{aligned}\tag{4.3}$$

The equations (4.1), (4.2) and (4.3) are rewritten to the rotation matrices R_ψ , R_θ and R_ϕ as

$$R_\psi = \begin{bmatrix} \cos(\psi) & \sin(\psi) & 0 \\ -\sin(\psi) & \cos(\psi) & 0 \\ 0 & 0 & 1 \end{bmatrix} R_\theta = \begin{bmatrix} \cos(\theta) & 0 & -\sin(\theta) \\ 0 & 1 & 0 \\ \sin(\theta) & 0 & \cos(\theta) \end{bmatrix} R_\phi = \begin{bmatrix} 1 & 0 & 0 \\ 0 & \cos(\phi) & \sin(\phi) \\ 0 & -\sin(\phi) & \cos(\phi) \end{bmatrix}\tag{4.4}$$

The transformation matrix T , from the local coordinate system $X_3 Y_3 Z_3$ to the global coordinate system $X_G Y_G Z_G$ where rotation has been carried out in yaw, pitch and roll angles are given by

$$T = R_\psi R_\theta R_\phi\tag{4.5}$$

Equation (4.5) and (4.4) give the the following transformation matrix from local to global coordinate system

$$T = \begin{bmatrix} \cos(\theta) \cos(\psi) & \cos(\theta) \sin(\psi) & -\sin(\theta) \\ \sin(\phi) \sin(\theta) \cos(\psi) - \cos(\phi) \sin(\psi) & \cos(\phi) \cos(\psi) + \sin(\phi) \sin(\theta) \sin(\psi) & \sin(\phi) \cos(\theta) \\ \sin(\phi) \sin(\psi) + \cos(\phi) \sin(\theta) \cos(\psi) & \cos(\phi) \sin(\theta) \sin(\psi) - \sin(\phi) \cos(\psi) & \cos(\phi) \cos(\theta) \end{bmatrix}\tag{4.6}$$

The transformation from global to local coordinate system is the transpose of equation (4.6). [2]

4.2 Chassis

The vehicle is a 6 degree of freedom body, with lateral-, longitudinal and vertical translation and rotation in pitch, roll and yaw as degrees of freedom. The vehicle is modeled as a two mass system where the vehicle body is the sprung mass and is seen as a rigid body with the mass centered in the center of gravity. The equations of motion of the Vehsim vehicle model are derived for translational motion in x- y- and z-direction and rotational motion around the vehicle body coordinate axis. [9]

4.2.1 Translational equations of motion

The equation of motion derived from Newtons second law, equation (3.2). The acceleration of the center of gravity is given by

$$\bar{a} = \dot{\bar{v}} + \bar{\omega} \times \bar{v} = \begin{bmatrix} \dot{v}_x \\ \dot{v}_y \\ \dot{v}_z \end{bmatrix} + \begin{vmatrix} \hat{x} & \hat{y} & \hat{z} \\ \omega_x & \omega_y & \omega_z \\ v_x & v_y & v_z \end{vmatrix} = \begin{bmatrix} \dot{v}_x + \omega_y v_z - \omega_z v_y \\ \dot{v}_y + \omega_z v_x - \omega_x v_z \\ \dot{v}_z + \omega_x v_y - \omega_y v_x \end{bmatrix} \quad (4.7)$$

The acceleration in the body fixed coordinate system is

$$\bar{a} = \frac{1}{m}(\bar{F}_{fl} + \bar{F}_{fr} + \bar{F}_{rl} + \bar{F}_{rr} - F_{drag} + m\bar{g}) \quad (4.8)$$

where \bar{F}_{fl} , \bar{F}_{fr} , \bar{F}_{rl} and \bar{F}_{rr} are the tire forces working on the vehicle body, $m\bar{g}$ is the gravitational force and F_{drag} is the aerodynamic drag force, given by

$$F_{drag} = \frac{1}{2}\rho A C_D V^2 \quad (4.9)$$

where ρ is the air density, A is the front area of the car, C_D is the drag coefficient and V is the body velocity. [9]

4.2.2 Rotational equations of motion

This section shows the derivation of the rotational equation of motion with Euler equations [2]. The sum of the moment around the center of mass is the total change of angular momentum.

$$\sum \bar{M} = \frac{d\bar{H}}{dt} \quad (4.10)$$

The angular momentum is

$$\bar{H} = \sum_i R_i \times m_i \frac{d\bar{R}_i}{dt}$$

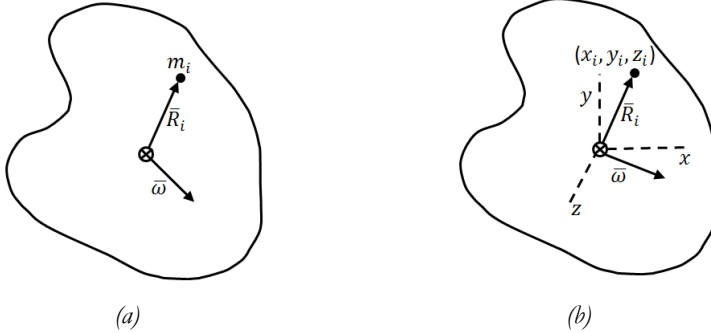


Figure 4.4: A rotating rigid body

where R_i is the distance from the center of gravity to i :th particle and m_i is the mass of the i :th particle, see *Figure 4.4a*. The i :th particle of the rigid body has velocity $d\bar{R}_i/dt = \bar{\omega} \times \bar{R}_i$ and angular momentum becomes

$$\bar{H} = \sum_i \bar{R}_i \times m_i (\bar{\omega} \times \bar{R}_i) \quad (4.11)$$

A new coordinate system with origo in center of mass is introduced, see *Figure 4.4b*, and \bar{R}_i and $\bar{\omega}$ can be expressed in this coordinate system as

$$\bar{\omega} = \omega_x \cdot \hat{e}_x + \omega_y \cdot \hat{e}_y + \omega_z \cdot \hat{e}_z \quad (4.12)$$

and

$$\bar{R}_i = x_i \cdot \hat{e}_x + y_i \cdot \hat{e}_y + z_i \cdot \hat{e}_z \quad (4.13)$$

Evaluating equation (4.12) and equation (4.13) in equation (4.11) gives the components of angular momentum

$$\begin{aligned} H_x &= I_{xx}\omega_x - I_{xy}\omega_y - I_{xz}\omega_z \\ H_y &= -I_{yx}\omega_x + I_{yy}\omega_y - I_{yz}\omega_z \\ H_z &= -I_{zx}\omega_x - I_{zy}\omega_y + I_{zz}\omega_z \end{aligned} \quad (4.14)$$

The Euler equations becomes

$$\begin{bmatrix} \sum M_x \\ \sum M_y \\ \sum M_z \end{bmatrix} = \begin{bmatrix} I_{xx} & -I_{xy} & -I_{xz} \\ -I_{yx} & I_{yy} & -I_{yz} \\ -I_{zx} & -I_{zy} & I_{zz} \end{bmatrix} \begin{bmatrix} d\omega_x/dt \\ d\omega_y/dt \\ d\omega_z/dt \end{bmatrix} + \begin{bmatrix} 0 & -\omega_z & \omega_y \\ \omega_z & 0 & -\omega_x \\ -\omega_y & \omega_x & 0 \end{bmatrix} \begin{bmatrix} I_{xx} & -I_{xy} & -I_{xz} \\ -I_{yx} & I_{yy} & -I_{yz} \\ -I_{zx} & -I_{zy} & I_{zz} \end{bmatrix} \begin{bmatrix} \omega_x \\ \omega_y \\ \omega_z \end{bmatrix} \quad (4.15)$$

The products of inertia are assumed to be zero, that is

$$I_{xz} = I_{zx} = I_{xy} = I_{yx} = I_{yz} = I_{zy} = 0 \quad (4.16)$$

The moments of inertia I_{xx} , I_{yy} and I_{zz} are calculated by approximating the vehicle as a rectangular box with sides *Length*, *Width* and *Height*, see *Figure 4.5*. The moments of inertia are

$$\begin{aligned} I_{xx} &= \frac{1}{12}m(Length^2 + Width^2) \\ I_{yy} &= \frac{1}{12}m(Length^2 + Height^2) \\ I_{zz} &= \frac{1}{12}m(Height^2 + Width^2) \end{aligned} \quad (4.17)$$

The sum of moments around the center of gravity is

$$\sum M = \bar{r}_{fl} \times \bar{F}_{fl} + \bar{r}_{fr} \times \bar{F}_{fr} + \bar{r}_{rl} \times \bar{F}_{rl} + \bar{r}_{rr} \times \bar{F}_{rr} \quad (4.18)$$

where \bar{r}_{fl} , \bar{r}_{fr} , \bar{r}_{rl} and \bar{r}_{rr} are the distances from the center of gravity to each wheel hub.

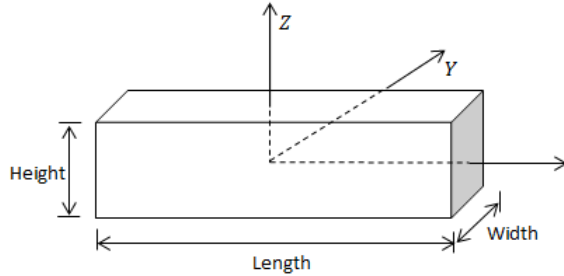
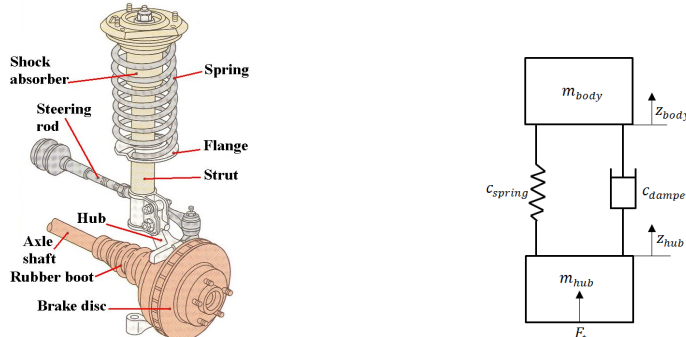
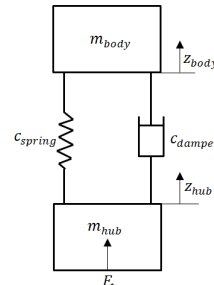


Figure 4.5: Moment of inertia of a rectangular box

4.2.3 Suspension



(a) MacPherson Strut



(b) Two mass spring damper system

The suspension of the Vehsim vehicle model is based on the MacPherson strut and it consists of a integrated shock absorber and coil spring, see *Figure 4.6a*. The MacPherson strut is simplified to a

two-mass spring damper system and the vertical force that acts on the vehicle body from the tires is obtained by making calculations on the spring damper system, see *Figure 4.6b*. The spring and the damper is in parallel since they share the same load. The mass of the vehicle body can be ignored with the assumption that the reference position for the displacement is a static equilibrium point. The equation of motion for one wheel is

$$F_t - (F_{spring} + F_{damper}) = m_{hub} \cdot \ddot{z}_{hub} \quad (4.19)$$

where F_t is the tire force, F_{spring} is the spring force and F_{damper} is the force from the damper. The spring force is given by

$$F_{spring} = c_{spring}(z_{body} - z_{hub}) \quad (4.20)$$

and the damper force by

$$F_{damper} = c_{damper}(\dot{z}_{body} - \dot{z}_{hub}) \quad (4.21)$$

Equation (4.21) is approximated with damping characteristics, see *Figure 4.7*.

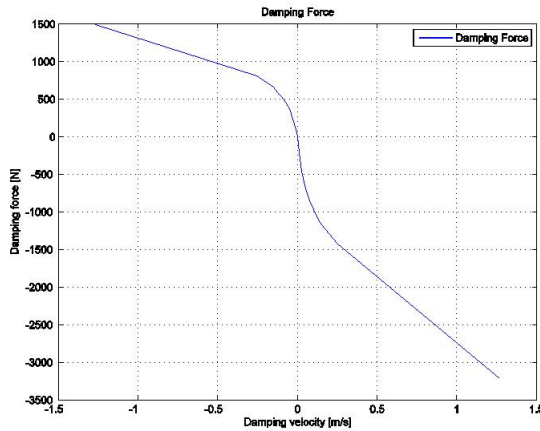


Figure 4.7: Damping Characteristics

4.2.4 Anti-roll bar

An anti-roll bar is used to stabilize the car in roll motion. The bar, which is connected to the car frame, is twisted when a difference in vertical position between left and right wheel occurs and works as torsion spring that reduces the roll. The Vehsim vehicle model has two anti-roll bars, one for the front- and one for the rear wheels. The anti-roll bar force is given by

$$F_{AntiRollBar} = c_{AntiRollBar}((z_{body} - z_{hub}) - (z_{body,opposite} - z_{hub,opposite})) \quad (4.22)$$

4.2.5 Steering kinematics

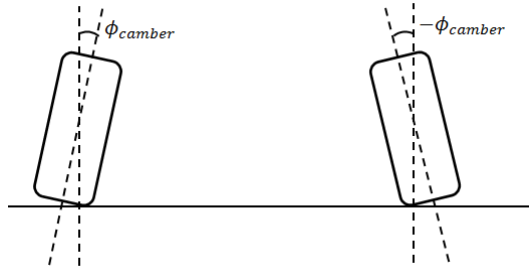


Figure 4.8: Camber Angle

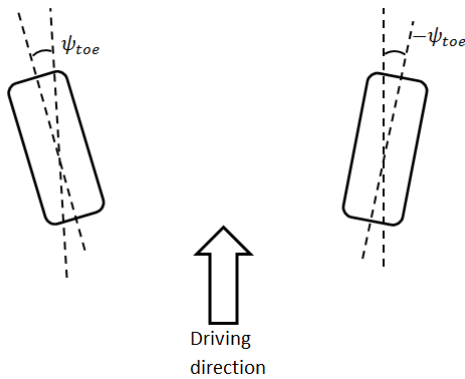


Figure 4.9: Toe Angle

Each wheel has a hub fixed coordinate system and the inclination of the wheel in this system is important for how the tire forces are transferred to the body coordinate system. The angles are

ϕ_{camber}	Camber	- rotation around X-axis
θ_{caster}	Caster	- rotation around Y-axis
ψ_{toe}	Toe	- rotation around Z-axis

The *Caster* angle is assumed to be zero in this model. The *Camber* and *Toe* angles have static components but the resulting angles are also affected by dynamical changes in z -direction and wheel steering angle δ . The *Camber* and *Toe* angles are given by

$$\phi_{camber} = \text{CamberSuspensionRatio} \cdot dz + \text{CamberSteerRatio} \cdot \delta + \text{StaticCamberAngle} \quad (4.23)$$

$$\psi_{toe} = \delta + \text{StaticToeAngle} + \text{BumpSteer} \cdot dz \quad (4.24)$$

Euler angles are used for transformations between the local wheel coordinate system and the body coordinate system, see 4.1.3 for derivation. The transformation matrix is given by equation (4.6) with ϕ_{camber} , θ_{caster} and ψ_{toe} as angles.

4.3 Tires in Vehsim vehicle model

The Magic Tire Formula is a semi-empirical model. A full description of the model can be found in Tyre and Vehicle Dynamics, see [1]. The model is based on mathematical expressions and describes the characteristics of the tires.

4.3.1 Pure Slip

The expression for lateral force F_y as a function of lateral slip α in pure slip is given by:

$$F_y = D \cdot \sin[C \cdot \arctan[B\alpha - E(\alpha - \arctan(B\alpha))]] \quad (4.25)$$

where the coefficients are

- D is the peak factor
- C is the shape factor
- B is the stiffness factor
- E is the curvature factor

The equation for longitudinal force F_x as a function of longitudinal slip κ is the same as equation (4.25) with F_y and α replaced by F_x and κ .

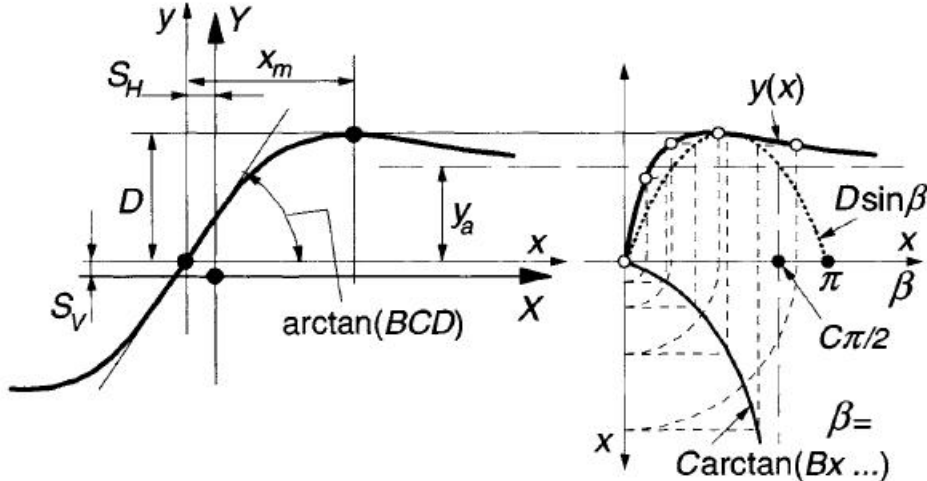


Figure 4.10: Magic tire formula, [1]

4.3.2 Combined Slip

Combined slip is when a lateral slip angle α decreases the force longitudinal force F_x and a longitudinal slip angle κ decreases the lateral force F_y . In the magic tire model combined slip is handled by multiplying equation (4.25) for pure slip with a weighting function given by

$$G = D \cdot \cos[C \cdot \arctan(Bx)] \quad (4.26)$$

5 | Measurements

The data used to optimize parameters and validate the models was collected by making measurements on a test car. The same tests were conducted both in summer and winter conditions to get low and high road friction data. The winter testing took place on Colmis proving ground in Arjeplog and the summer testing at Ljungbyhed.



Figure 5.1: The test car, a Volkswagen Golf 7, 4MOTION

5.1 Test car data

The test car was a Volkswagen Golf 7, 4MOTION and the same car, but with different tires was, used on both test occasions, see *Figure 5.1* for a picture and *Table 5.1* for car specific data.

mass	1400 kg
Length	4.255 m
Width	1.799 m
Length between wheels	2.637 m
Width between wheels front	1.549 m
Width between wheels rear	1.52 m

Table 5.1: Car specific data for the test Golf

5.2 Test maneuvers

Different type of maneuvers were conducted to use for validation of the vehicle. A short description of each maneuver follows.

5.2.1 Offset Run

The *Offset run* was done by accelerate from rest and drive straight forward. This data is used for calculating offsets in the sensor measurements.

5.2.2 Step with gear in neutral position

The *Step with gear in neutral position* run started at a speed around 100 km/h and then the gear was set to neutral position and steps in steering angles was applied. The reason to put the gear in neutral position was that then there is no driving force on the wheels and the data can be used to optimize tire parameters.

5.2.3 Step in steer angle

The goal of the *Step in steering angle* maneuver was to get the car into steady state. The run started at constant speed and then steps in steering angle was applied, this was done for different speeds.

5.2.4 Sinus driving

The *Sinus driving* measurement was done by driving in constant speed and then steer the car as a sinusoidal wave. This was done for different speeds.

5.2.5 Handling tracks

Data from the *Handling tracks* measurements are used to validate the model after using other data to optimize parameters. The two handling tracks on the winter testing facility can be seen to the left in *Figure 5.2*.



Figure 5.2: Colmis proving ground in Arjeplog [4]

5.3 Measurement equipment

The embedded CAN-bus of the car and external sensors for acceleration and velocity measurements were used. The reason to have external measurement equipment was the possibility to be able to filter the signals. The signals from the embedded CAN-bus are already filtered but the level of filtering is unknown. The CAN-bus was used for *yaw rate*, *steering angle*, *wheel speed* and *lateral acceleration* data.

5.3.1 Accelerometer



Figure 5.3: Motion sensor with accelerometer

A motion sensor with integrated accelerometer was placed between the two front seats to measure *longitudinal acceleration*. The sensor used for measurements comes from Omni instruments and the model which is called LPMS-CU is a 9-axis IMU AHRS motion sensor see *Figure 5.3*.

5.3.2 Optical velocity sensor

The velocity data was measured with an optical sensor called Correvit s-350 Aqua from Kistler. The sensor was mounted at the front of the car 0.35 m above the ground, see *Figure 6.2*.



Figure 5.4: The optical velocity sensor mounted on the test car

6 | Simulation

The tool used for the simulations is Matlab Simulink and the two models simulated are the bicycle model described in *Chapter 3* and the complete vehicle model from Vehsim in *Chapter 4*. Measurement data from the tests in *Chapter 5* are read into the models. The simulations uses a fixed time step solver in Simulink called ode2 (Heun) with a fixed time step of 0.002s

6.1 Signals

The measurement signals used in the models are *lateral acceleration*, *longitudinal acceleration*, *lateral velocity*, *longitudinal velocity*, *steering angle*, *wheel rotational speed*, *wheel speed*, *yaw rate* and *yaw acceleration*. The measurement data from *Chapter 5* must be processed before it can be used in the Matlab simulations. The processing includes filtering the measurement signals and taking out important values in the measurement files to use for the optimizations.

6.1.1 Filtering of measurement signals

The signals from the CAN-bus are already filtered but the signals from the other sensors are filtered with a low pass filter to reduce the noise in the measurements.

6.1.2 Accelerations

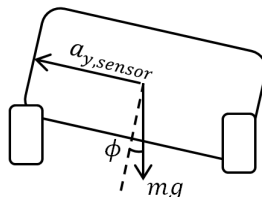


Figure 6.1: The acceleration sensor signals is affected by gravity

The accelerometer was not exactly placed in the center of gravity during measurements and due to that, an offset in the measurements must be calculated and compensated for in the simulations. The sensor data for lateral acceleration is also affected by gravity, see *Figure 6.1*. The lateral acceleration

is given by

$$a_y = a_{y,sensor} - mg \cdot \sin(\phi) \quad (6.1)$$

where $a_{y,sensor}$ is the measured value of lateral acceleration and ϕ is the roll angle.

6.1.3 Velocities

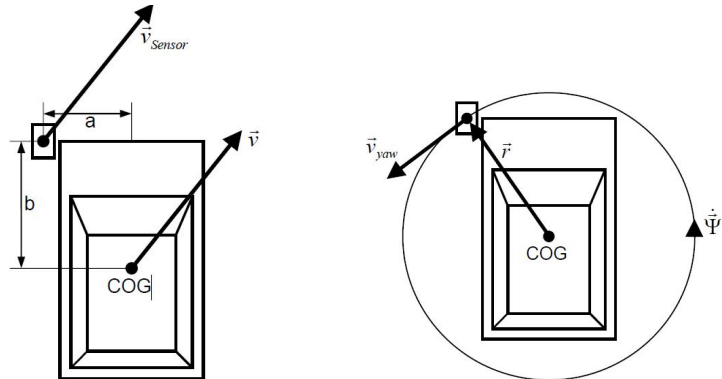


Figure 6.2: Placement of velocity sensor relative center of gravity of the car

Lateral and longitudinal velocities are sampled using the optical velocity sensor in Section 5.3.2. The output signals from the velocity sensor are total velocity v_{sensor} and the sensor angle γ . The signals are filtered through a low pass filter to reduce noise and the offset in γ is calculated. Lateral and longitudinal velocity is calculated with

$$\begin{aligned} v_x &= v_{sensor} \cdot \cos(\gamma) \\ v_y &= v_{sensor} \cdot \sin(\gamma) \end{aligned} \quad (6.2)$$

Figure 6.2 shows the location of the velocity sensor relative the center of gravity. The lateral and longitudinal velocity in the center of gravity is calculated from the sensor velocities with

$$v_x = v_{sensor,x} + \dot{\psi} \cdot a \quad (6.3)$$

$$v_y = v_{sensor,y} - \dot{\psi} \cdot b \quad (6.4)$$

where a is the lateral distance from the center of gravity to the velocity sensor, b is the longitudinal distance from the center of gravity to the velocity sensor and $\dot{\psi}$ is the yaw rate of the vehicle.

6.1.4 Wheel rotation and wheel speed

The wheel speed and wheel rotational speed signals comes from the CAN-bus and no further filtering is needed.

6.1.5 Yaw Rate and and Yaw Acceleration

The yaw rate signal is taken from the CAN-bus and the yaw acceleration is calculated using a filter in Simulink that returns the derivative of the signal.

6.1.6 Steering Angle

The steering angle signal comes from the CAN-bus and an offset is calculated and used in the simulations. Steering angle data is transformed to wheel angle δ by the look-up table in *Table 6.1*, intermediate angles are interpolated. The look-up table is not valid above 8.8 rad .

Steering Angle [rad]	Wheel Angle [rad]
MAX	1.99
8.83	0.6423
6.458	0.4423
3.229	0.2138
1.361	0.0896
MIN	0.0

Table 6.1: Look-up table for transformation between steering angle and wheel angle

6.2 Simulation of bicycle model

Inputs to the bicycle model are *Wheel angle*, *Lateral velocity*, *Longitudinal velocity* and *Yaw rate*. The outputs *Yaw acceleration* and *Lateral acceleration* are compared with measurement data. The Simulink model can be seen in *Figure 6.3*

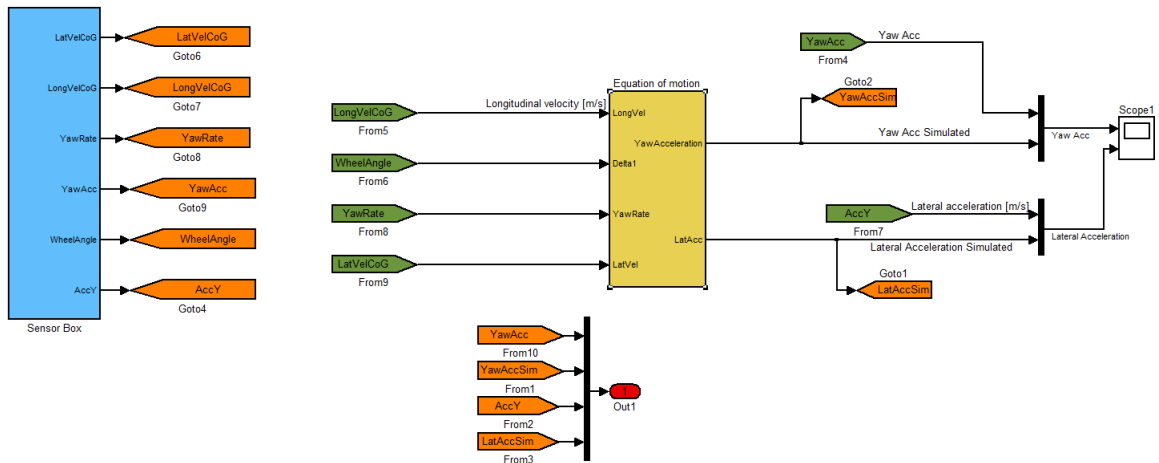


Figure 6.3: Bicycle model in Simulink

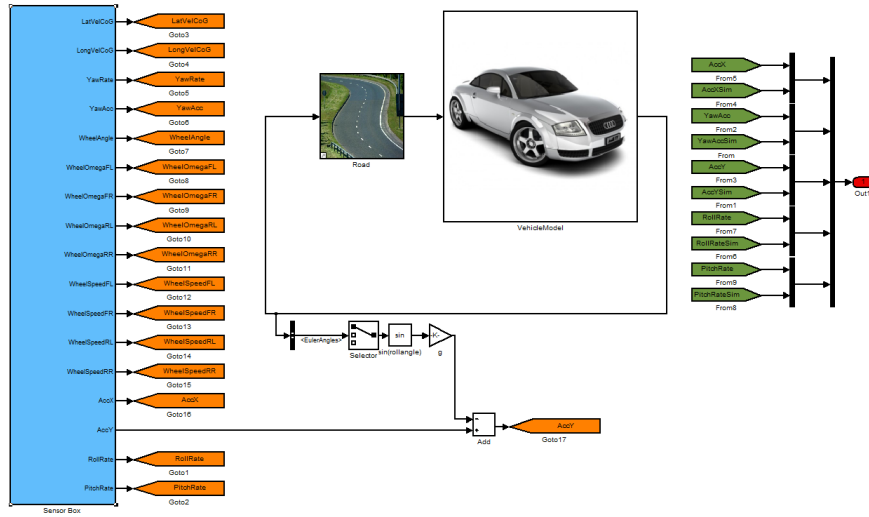


Figure 6.4: Vehsim vehicle model

6.3 Simulation of Vehsim vehicle model for optimization of parameters

The simulated vehicle model used for optimization of tire and chassis parameters is simplified compared to the original vehicle model in Vehsim described in *Chapter 2*. Some calculations of signals have been replaced with measured data. The Simulink model can be seen in *Figure 6.4* and *Table 6.2* shows the input and output signals used in the optimization. Measurement data are read into the model from the sensor box to the left in the picture and simulated data outputs can be seen to the right in the picture. The simulation contains the modules, *Road* and *Vehicle*, the output of the road model is road friction and the vehicle model is built of *Chassis* and *Tire* modules. *Figure 6.5* shows how measurement data is integrated in the calculation loop.

<i>Input signals</i>	<i>Output signals</i>
Lateral velocity	Longitudinal acceleration
Longitudinal velocity	Yaw acceleration
Lateral acceleration	Lateral acceleration
Longitudinal acceleration	
Yaw rate	
Steering angle	
Wheel speed	
Wheel rotational speed	

Table 6.2: Inputs and outputs of Vehsim vehicle model

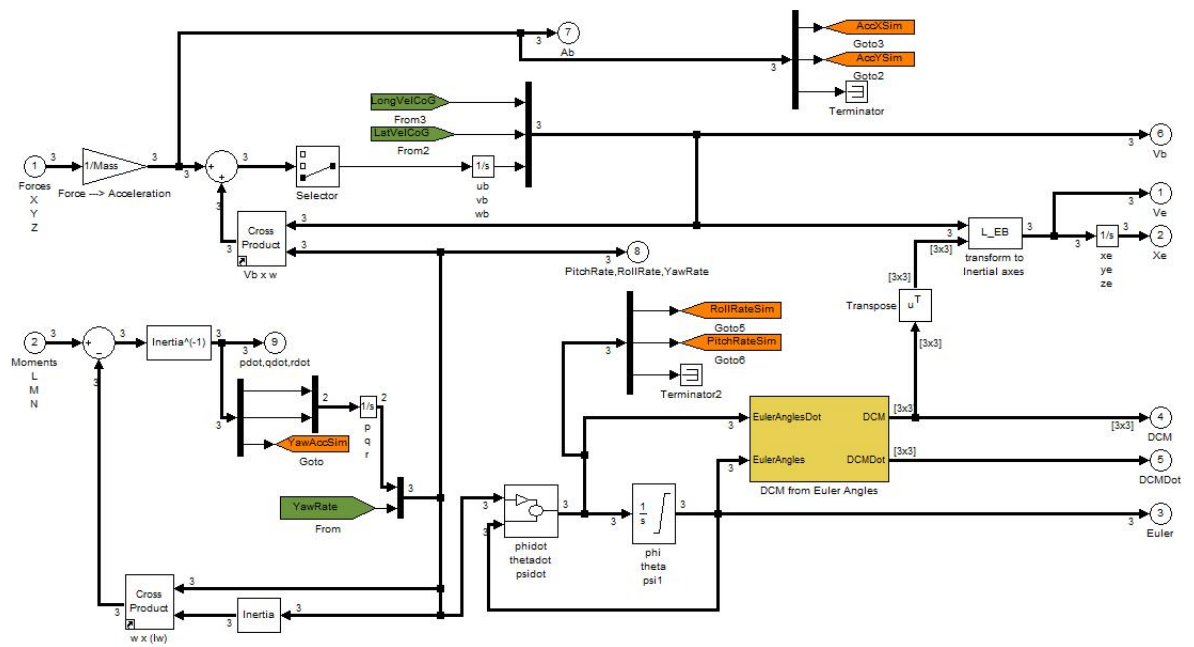


Figure 6.5: Integration of measurement data in the vehicle model

7 | Optimization and validation

The different parameters are optimized by minimizing the error between simulated and measured data using the *lsqnonlin* command in Matlab and run the simulation in every iteration.

7.1 Theory of optimization part

The Matlab command *lsqnonlin*, included in the optimization toolbox, is used to optimize the parameters in the vehicle models. This function uses a least square method to solve non-linear data fitting problems on the form

$$\min_x \|f\|_2^2 = \min_x (f_1(x)^2 + f_2(x)^2 + \dots + f_n(x)^2) \quad (7.1)$$

The Matlab function needs the following input from the user

$$f(x) = \begin{bmatrix} f_1(x) \\ f_2(x) \\ \vdots \\ f_n(x) \end{bmatrix} \quad (7.2)$$

where f_i in this case is given by

$$f_i = \gamma_i \cdot e_i \quad (7.3)$$

The scaling factor, γ_i is described in section 7.3 and the error, e_i in each measuring point, i is given by

$$e_i = y_{i,\text{measured}} - y_{i,\text{simulated}} \quad (7.4)$$

where the parameters $y_{i,\text{measured}}$ and $y_{i,\text{simulated}}$ are the measured and simulated values of the signal. The optimizations are solved without constraints and the discretization is the same as in the Simulink models. A limitation of *lsqnonlin* is that the solution might be a local minimum [5].

7.1.1 Error

A total error, ϵ is calculated to have a measurable value to use for comparison between the runs of the optimization. The error is calculated as the Euclidean norm of the difference between measured and simulated data.

$$\epsilon = \sqrt{\sum_i |e_i|^2} \quad (7.5)$$

7.2 Preparation of measurement files for optimization

The measurement files that are used in the simulations needs some preparation before the actual optimization can be done. This section describes for example the offset calculations, how optimization indices is chosen and how the scaling parameter is calculated.

7.2.1 Offset calculations

Sensor offset values are calculated for *Lateral-* and *Longitudinal acceleration*, *Steering angle* and *Velocity sensor angle*. The offset values are calculated as the mean sensor value when the total velocity is close to zero, that is when the velocity is smaller than $0.0001m/s$.

7.2.2 Add measurement files

The Matlab script used for minimization of simulation error are built to handle data from more than one measurement file. The data from the chosen test runs are put after each other and then simulated as one measurement file.

7.2.3 Optimization index

The parameters are fitted by solving an optimization problem where the error between measured and simulated data is minimized. The minimizing algorithm only uses the part of the measurement data where the velocity is greater than 20 km/h, this is to avoid sensor related problems in the starting phase.

7.2.4 Steady state index for tire optimization

The magic tire formula is only valid in steady state and therefore measurement data for step input in steering angle was used to optimize tire parameters. The steady state indices was found looking at lateral- and yaw acceleration and then used for tire parameter optimization, see *Figure 7.1*.

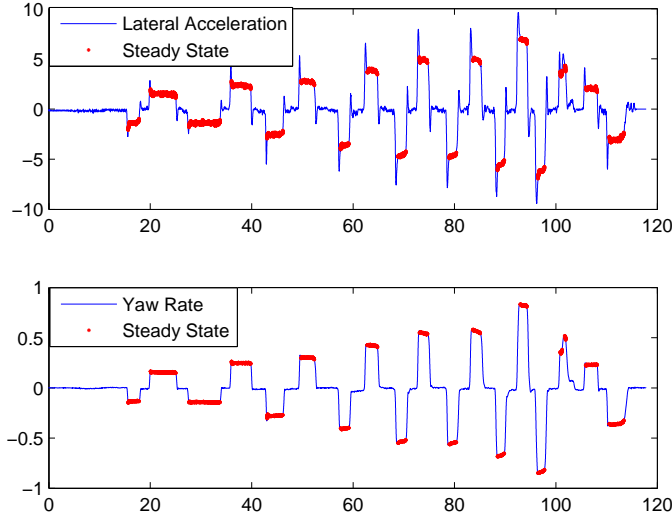


Figure 7.1: Measurement data of lateral- and yaw acceleration with steady state indices

7.2.5 Scaling

During the optimization of parameters both yaw- and lateral acceleration data are considered and since they are of different size a scaling factor must be calculated to get a result where all data is of equal importance in the optimization. The scaling factor γ_{LatAcc} is

$$\gamma_{LatAcc} = 1 \quad (7.6)$$

and γ_{YawAcc} is calculated as the fraction between mean values of absolute values of measured lateral- and yaw acceleration data that is greater than 0.5, i.e

$$\gamma_{YawAcc} = \frac{\text{mean}(|y_{i,LatAccMeasured}| > 0.5m/s^2)}{\text{mean}(|y_{i,YawAccMeasured}| > 0.5rad/s^2)} \quad (7.7)$$

7.3 Bicycle model parameters optimization

The optimized parameters in the bicycle model are the tire coefficients C_{12} , C_{34} . The optimization is solved with measurement and simulated data for lateral acceleration and yaw acceleration.

Equation 7.2 for the bicycle optimization is given by

$$f = \begin{bmatrix} \gamma_{LatAcc} \cdot (y_{1,LatAccMeasured} - y_{1,LatAccSimulated}) \\ \vdots \\ \gamma_{LatAcc} \cdot (y_{n,LatAccMeasured} - y_{n,LatAccSimulated}) \\ \gamma_{YawAcc} \cdot (y_{1,YawAccMeasured} - y_{1,YawAccSimulated}) \\ \vdots \\ \gamma_{YawAcc} \cdot (y_{n,YawAccMeasured} - y_{n,YawAccSimulated}) \end{bmatrix} \quad (7.8)$$

where $i = 1 \dots n$ are the optimization indices described in section 7.2.3 and $y_{i,LatAccMeasured}$, $y_{i,YawAccMeasured}$, $y_{i,YawAccSimulated}$ and $y_{i,LatAccSimulated}$ are the measured and simulated values of the lateral- and yaw acceleration for those indices. The scaling parameters γ_{LatAcc} and γ_{YawAcc} are described in

7.4 Optimization of Vehsim vehicle model parameters

The optimization of parameters in the Vehsim vehicle model is done in three steps. The radius of the wheels is optimized first, then the tire parameters and last the chassis parameters. The reason to divide the optimization is that the values of some of the resulting parameters where unreasonable when all parameters were fitted in one optimization.

7.4.1 Wheel radius optimization

The wheel radius is one of the tire parameters that can be set but it is optimized separately since it is fitted to data for longitudinal acceleration instead of lateral- and yaw acceleration. To find the radius of the wheel, the error between measured and simulated data for longitudinal acceleration is minimized using *lsqnonlin*. The measurements data comes from *Offset run*. *Equation 7.2* for the wheel radius optimization is given by

$$f = \begin{bmatrix} (y_{1,LongAccMeasured} - y_{1,LongAccSimulated}) \\ \vdots \\ (y_{n,LongAccMeasured} - y_{n,LongAccSimulated}) \end{bmatrix} \quad (7.9)$$

where $i = 1 \dots n$ are all available indices in the *Offset run* measurement file and $y_{i,LongAccMeasured}$ and $y_{i,LongAccSimulated}$ are the measured and simulated values of longitudinal acceleration.

7.4.2 Tire parameters optimization

The tire parameters are optimized using steady state indices for lateral- and yaw acceleration. The tire parameters optimized are road friction for front wheel, *LMUF*, road friction for rear wheel,

$LMUR$, tire stiffness in lateral direction for front wheel, $LKYAF$ and for rear wheel, $LKYAR$. Equation 7.2 for the tire optimization is given by

$$f = \begin{bmatrix} \gamma_{LatAcc} \cdot (y_{1,LatAccMeasured} - y_{1,LatAccSimulated}) \\ \vdots \\ \gamma_{LatAcc} \cdot (y_{n,LatAccMeasured} - y_{n,LatAccSimulated}) \\ \gamma_{YawAcc} \cdot (y_{1,YawAccMeasured} - y_{1,YawAccSimulated}) \\ \vdots \\ \gamma_{YawAcc} \cdot (y_{n,YawAccMeasured} - y_{n,YawAccSimulated}) \end{bmatrix} \quad (7.10)$$

where $i = 1 \dots n$ are the steady state optimization indices described in section 7.2.4

7.4.3 Chassis parameters optimization

The tire parameters are optimized before the chassis parameters and the optimal values of the tire parameters are used in the chassis parameter optimization. Different combinations of the parameters found in Table 7.1 are optimized and the result is presented in Chapter 8. The input to *lsqnonlin* in the chassis parameter optimization is similar to Equation 7.8.

Tire Parameters	Chassis Parameters
Road friction front wheel, LMUF	Toe angle front wheel
Road friction rear wheel, LMUR	Toe angle rear wheel
Lateral tire stiffness front wheel, LKYAF	Camber angle front wheel
Lateral tire stiffness rear wheel, LKYAR	Camber angle rear wheel
	Camber steer ratio front
	Camber suspension ratio front
	Camber suspension ratio rear
	Bump steer front
	Bump steer rear

Table 7.1: Chassis and tire parameters for the Vehsim vehicle model

7.5 Validation

After optimizing the model parameters a validation is made by simulating the model with optimal parameters and data from *Handling tracks* measurements. This is done both for the bicycle model and the Vehsim vehicle model.

8 | Results

This chapter shows the resulting plots and parameter values from the Simulink optimizations described in *Chapter 7*. The time it takes to solve the optimizations varies from under a minute for the simple bicycle model up to around 20 minutes for the chassis optimization of the Vehsim vehicle model with maximum number of parameters.

8.1 Result of bicycle model optimization

The tire parameters C_{12} and C_{34} are optimized using data in *Table 8.1*. The optimal parameter values are seen in *Table 8.2*. The result of the bicycle model simulated with optimal tire parameters and data from *Handling tracks* measurements are presented in *Figure 8.1* for high road friction, and in *Figure 8.2* for low road friction.

<i>Data, high road friction</i>	<i>Data, low road friction</i>
Step Input 30km/h	Step Input 50km/h
Step Input 90km/h	StepInput 110km/h

Table 8.1: Measurement data used to optimize bicycle tire parameters

<i>Parameter name</i>	<i>Parameter value , high road friction</i>	<i>Parameter value , low road friction</i>
C_{12}	53000 [N/rad]	9900 [N/rad]
C_{34}	95000 [N/rad]	13000[N/rad]
Error	890	1900

Table 8.2: Values of optimal tire parameters C_{12} and C_{34} for bicycle model

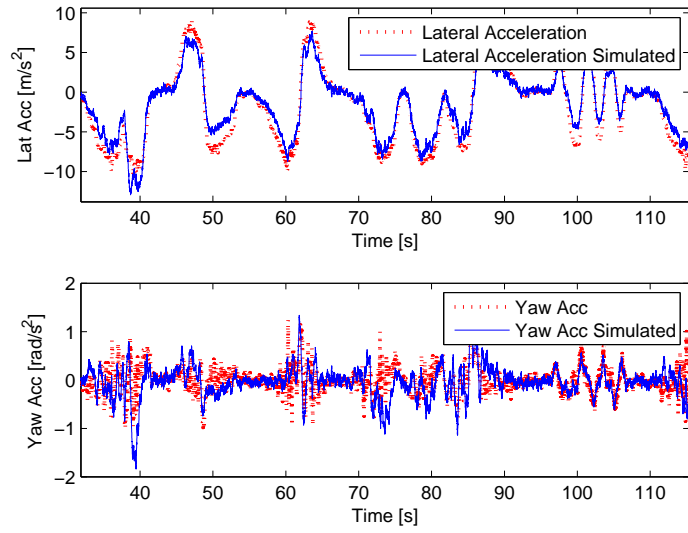


Figure 8.1: Simulation of bicycle model with optimal values of C_{12} and C_{34} and measurement data from handling tracks driving, high road friction

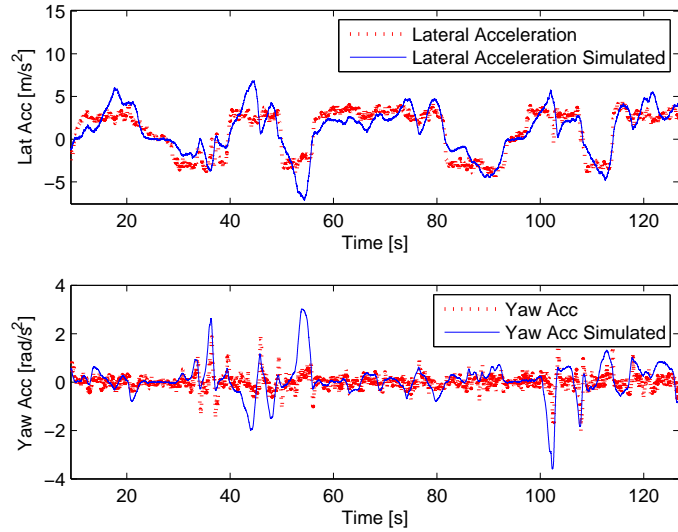


Figure 8.2: Simulation of bicycle model with optimal values of C_{12} and C_{34} and measurement data from handling tracks driving, low road friction

8.2 Result of wheel radius optimization for Vehsim vehicle model

The wheel radius optimization is based on data for longitudinal acceleration from *Offset Run* measurements. The wheel radius R_0 is optimized for both high and low road friction, the results can be seen in *Figure 8.3* and *8.4* and parameter values in *Table 8.3*.

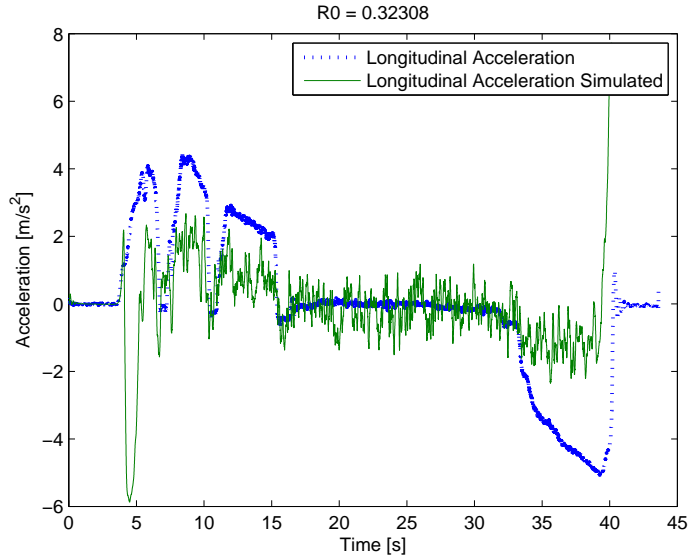


Figure 8.3: Result of wheel radius optimization based on longitudinal data from offset driving, high road friction

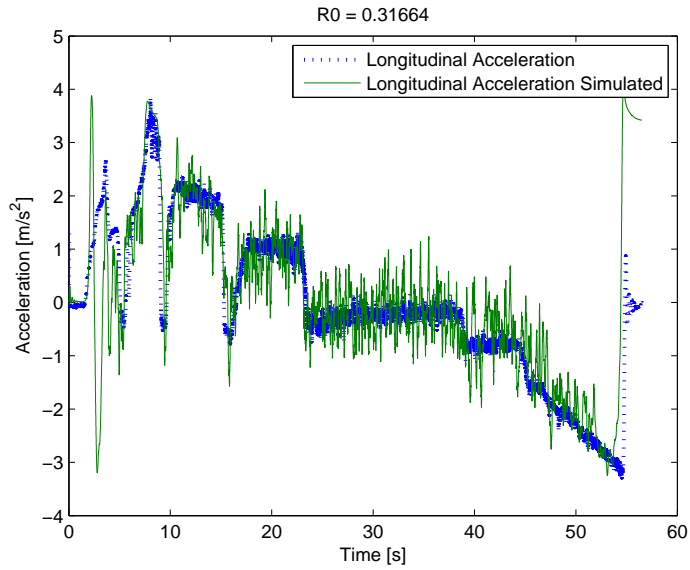


Figure 8.4: Result of wheel radius optimization based on longitudinal data from offset driving, low road friction

Data	Parameter name	Parameter value, high road friction	Parameter value, low road friction
Offset Run	R_0	0.323 [m]	0.317 [m]

Table 8.3: Parameter value of optimized wheel radius R_0 for high and low road friction

8.3 Result of Vehsim vehicle model tire parameters optimization

The tire scaling parameters $LMUF$, $LMUR$, $LKYAF$ and $LKYAR$ are optimized based on lateral- and yaw acceleration data from *Step with gear in neutral position* measurements. The measured and simulated data with optimized tire parameters for high and low road friction can be seen in Figure 8.5 and 8.6. The values of the tire scaling parameters for high and low road friction can be found in Table 8.4.

Data	Parameter name	Parameter value, high road friction	Parameter value, low road friction
Step with neutral gear	$LMUF$	1.06	0.47
	$LMUR$	1.0	0.43
	$LKYAF$	1.02	0.65
	$LKYAR$	2.04	0.71

Table 8.4: Optimal values of tire parameters for Vehsim vehicle model

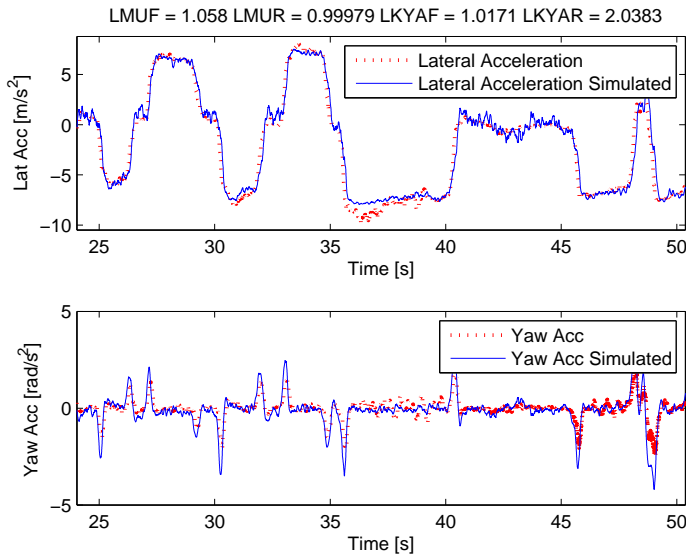


Figure 8.5: Result of optimization of tire parameters for Vehsim vehicle model, high road friction. Data from *Step with gear in neutral position* measurements

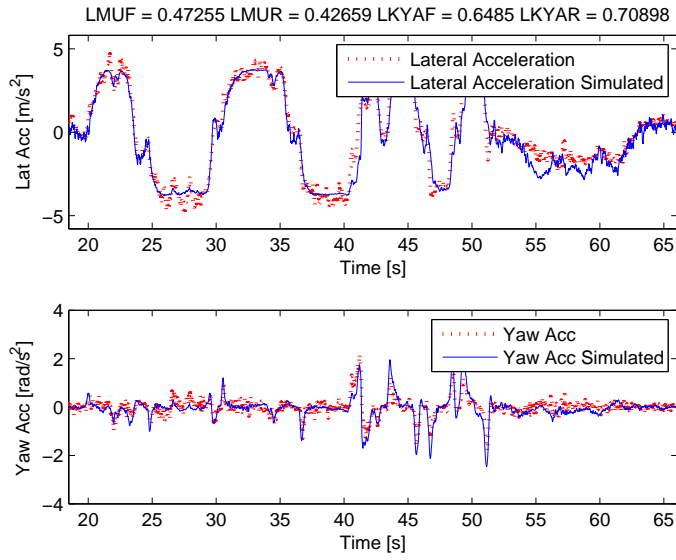


Figure 8.6: Result of optimization of tire parameters for Vehsim vehicle model, low road friction. Data from Step with gear in neutral position measurements

8.4 Optimization of chassis parameters

The chassis parameters *Static Camber Angle*, *Bump Steer*, *Static Toe Angle*, *Camber Suspension Ratio* and *Camber Steer Ratio* for front and rear wheels are optimized in different combinations. The tire scaling parameters are the same as in Section 8.3.

8.4.1 Static Camber Angle and Bump Steer

The *Static Camber Angle* and *Bump Steer* chassis parameters for front and rear wheels are optimized using measurement data seen in Table 8.5 and the resulting optimal parameter values for high and low road friction are seen in Table 8.6. Figure 8.7 and Figure 8.8 compares measurement data from *Handling tracks driving* with the result of a simulation with optimal parameter values of *Static Camber Angle* and *Bump Steer* for high and low road friction.

Data, high road friction	Data, low road friction
Step 30 km/h	StepInput 50 km/h
Step 90 km/h	StepInput 110 km/h
Sinus 50km/h	Sinus 30 km/h
Sinus 70 km/h	Sinus 70 km/h
Sinus 90 km/h	Sinus 90 km/h

Table 8.5: Data used for optimization of Static Camber Angle and Bump Steer

Parameter name	Parameter value, high road friction	Parameter name, low road friction
Static Camber Angle Front	0.02 [rad]	0.07[rad]
Static Camber Angle Rear	-0.01 [rad]	0 [rad]
Bump Steer Front	0.05 [rad/m]	0.96 [rad/m]
Bump Steer Rear	0.2 [rad/m]	1.05 [rad/m]
Error	1500	2070

Table 8.6: Optimal Static Camber Angle and Bump Steer parameters for Vehsim vehicle model with measurement data from step and sinus driving

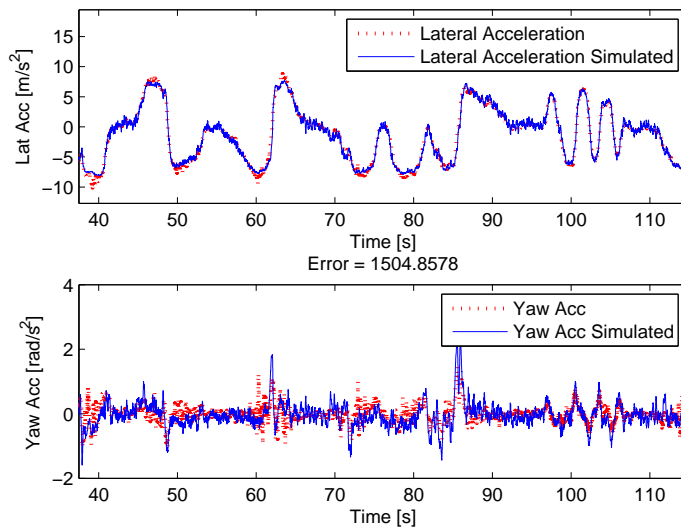


Figure 8.7: Simulation of Vehsim vehicle model with optimal values of Static Camber Angle and Bump Steer parameters and measurement data from handling track driving, high road friction.

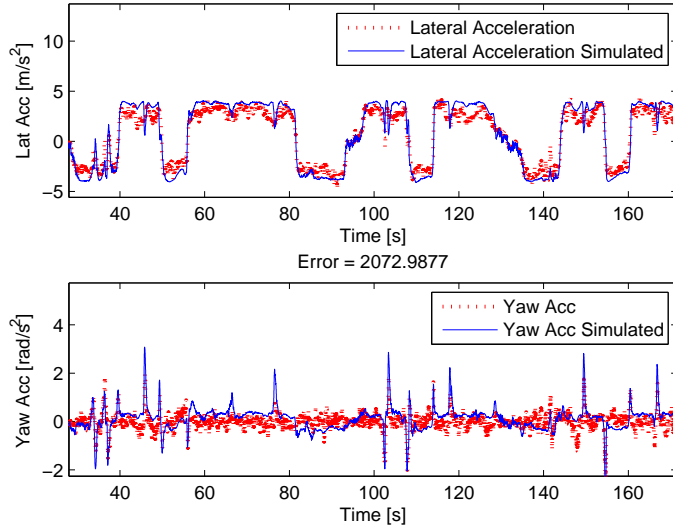


Figure 8.8: Simulation of Vehsim vehicle model with optimal values of Static Camber Angle and Bump Steer parameters and measurement data from handling track driving, low road friction.

8.4.2 Static Camber Angle, Bump Steer and Static Toe Angle

The chassis parameters *Static Camber Angle*, *Bump Steer* and *Static Toe Angle* are optimized using measurement data seen in *Table 8.7* and the optimal parameter values can be seen in *Table 8.8*. The Vehsim vehicle model is simulated with *Handling tracks driving* data and optimal values of *Static Camber Angle*, *Bump Steer* and *Static Toe Angle* and the result is compared with measurement data, see *Figure 8.9* for high road friction result and *Figure 8.10* for low road friction result.

<i>Data, high road friction</i>	<i>Data, low road friction</i>
Step 30 km/h	StepInput 50 km/h
Step 90 km/h	StepInput 110 km/h
Sinus 50 km/h	Sinus 30 km/h
Sinus 70 km/h	Sinus 70 km/h
Sinus 90 km/h	Sinus 90 km/h

Table 8.7: Data used for optimization of Static Camber Angle, Bump Steer and Static Toe Angle

Parameter name	Parameter value, high road friction	Parameter value, low road friction
Static Camber Angle Front	0.05 [rad]	0.11 [rad]
Static Camber Angle Rear	0.08 [rad]	0.08 [rad]
Bump Steer Front	0.50 [rad/m]	1.38 [rad/m]
Bump Steer Rear	-0.47 [rad/m]	-0.60 [rad/m]
Static Toe Angle Front	-0.01 [rad]	0 [rad]
Static Toe Angle Rear	-0.06 [rad]	-0.05 [rad]
Error	1400	1750

Table 8.8: Optimal Static Camber Angle, Bump Steer and Static Toe Angle parameters for Vehsim vehicle model with measurement data from step and sinus driving

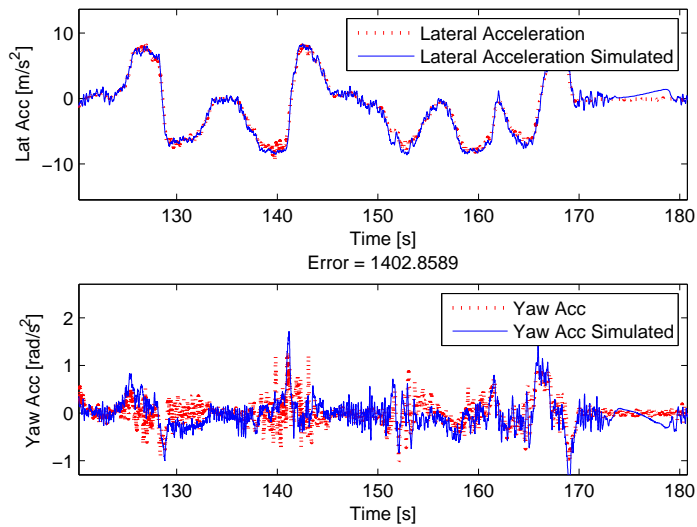


Figure 8.9: Simulation of Vehsim vehicle model with optimal values of Static Camber Angle, Bump Steer and Static Toe Angle parameters and measurement data from handling track driving, high road friction.

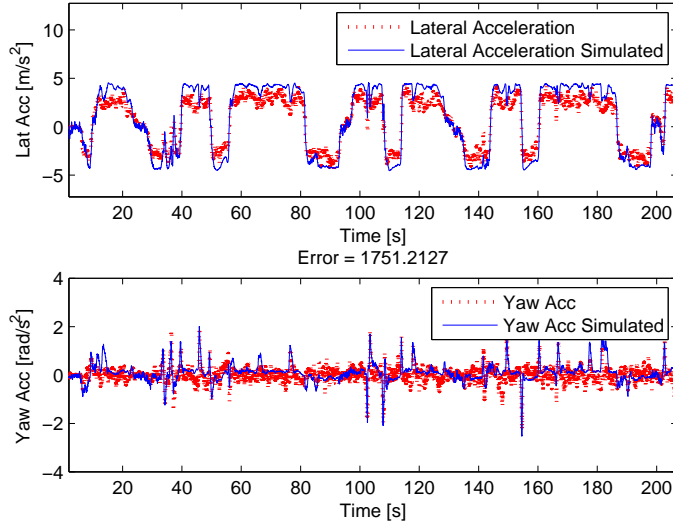


Figure 8.10: Simulation of Vehsim vehicle model with optimal values of Static Camber Angle, Bump Steer and Static Toe Angle parameters and measurement data from handling track driving, low road friction.

8.4.3 Static Camber Angle, Bump Steer, Static Toe Angle and Camber Suspension Ratio

The chassis parameters *Static Camber Angle*, *Bump Steer*, *Static Toe Angle* and *Camber Suspension Ratio* for front and rear wheel are optimized using the measurement data seen in *Table 8.9* and the optimal parameter values are seen *Table 8.10*. The optimal parameter values are used to simulate the Vehsim vehicle model with measurement data from *Handling tracks driving*, *Figure 8.11* and *8.12* shows high and low road friction simulation results compared with measurement data.

<i>Data, high road friction</i>	<i>Data, low road friction</i>
Step 30 km/h	StepInput 50 km/h
Step 90 km/h	StepInput 110 km/h
Sinus 50 km/h	Sinus 30 km/h
Sinus 70 km/h	Sinus 70 km/h
Sinus 90 km/h	Sinus 90 km/h

Table 8.9: Data used for optimization of Static Camber Angle, Bump Steer, Static Toe Angle and Camber Suspension Ratio

Parameter name	Parameter value, high road friction	Parameter value, low road friction
Static Camber Angle Front	0.09 [rad]	0.12 [rad]
Static Camber Angle Rear	0.06 [rad]	0.07 [rad]
Bump Steer Front	0.23 [rad/m]	0.73 [rad/m]
Bump Steer Rear	-0.05 [rad/m]	-0.63 [rad/m]
Static Toe Angle Front	0 [rad]	0 [rad]
Static Toe Angle Rear	-0.06 [rad]	-0.05 [rad]
Camber Suspension Front	-1.07 [rad/m]	-2.70 [rad/m]
Camber Suspension Rear	3.29 [rad/m]	0.50 [rad/m]
Error	1370	1700

Table 8.10: Optimal Static Camber Angle, Bump Steer, Static Toe Angle and Camber Suspension Ratio parameters for Vehsim vehicle model with measurement data from step and sinus driving

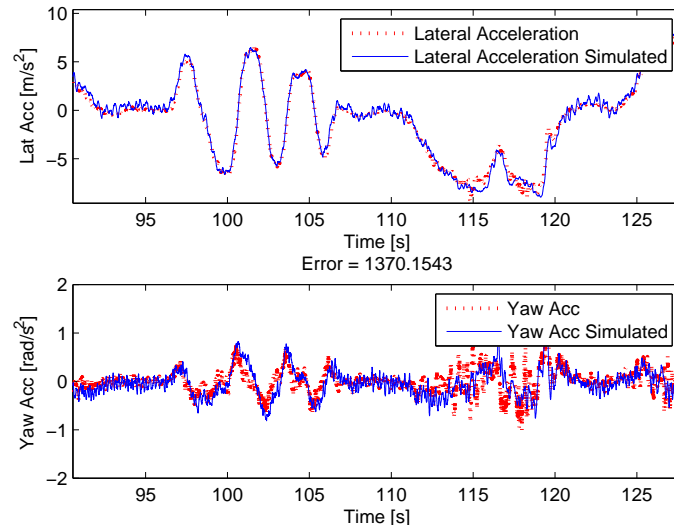


Figure 8.11: Simulation of Vehsim vehicle model with optimal values of Static Camber Angle, Bump Steer, Static Toe Angle and Camber Suspension Ratio parameters and measurement data from handling track driving, high road friction.

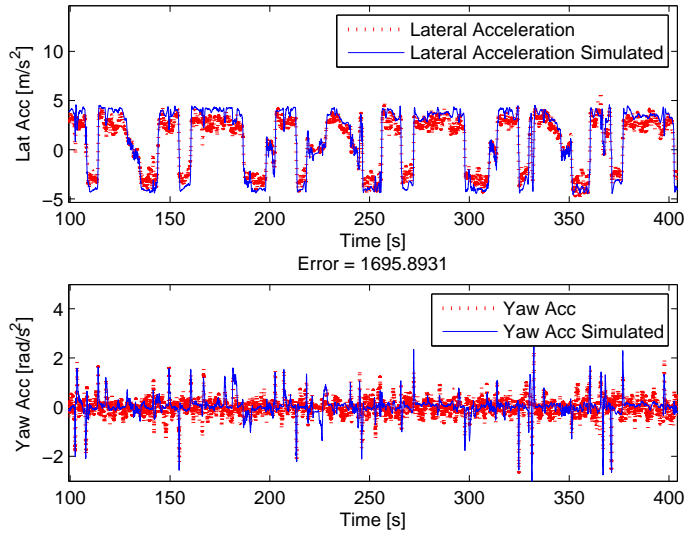


Figure 8.12: Simulation of Vehsim vehicle model with optimal values of Static Camber Angle, Bump Steer, Static Toe Angle and Camber Suspension Ratio parameters and measurement data from handling track driving, low road friction.

8.4.4 Static Camber Angle, Bump Steer, Static Toe Angle, Camber Suspension Ratio and Camber Steer Ratio

The measurement data seen in *Table 8.11* are used to optimize the chassis parameters *Static Camber Angle*, *Bump Steer*, *Static Toe Angle* and *Camber Suspension Ratio* for both front and rear wheel and also *Camber Steer Ratio* for front wheel. The optimal chassis parameter values, seen in *Table 8.12* are used to simulate the Vehsim vehicle model with measurement data from *Handling tracks driving*, the result of high and low road friction simulation compared with measurement data can be seen in *Figure 8.13* and *8.14*.

Data, high road friction	Data, low road friction
Step 30 km/h	StepInput 50 km/h
Step 90 km/h	StepInput 110 km/h
Sinus 50 km/h	
Sinus 70 km/h	
Sinus 90 km/h	

Table 8.11: Data used for optimization of Static Camber Angle, Bump Steer, Static Toe Angle, Camber Suspension Ratio and Camber Steer Ratio

Parameter name	Parameter value, high road friction	Parameter value, low road friction
Static Camber Angle Front	0.02 [rad]	0.04 [rad]
Static Camber Angle Rear	0.06 [rad]	0.01 [rad]
Bump Steer Front	0.21 [rad/m]	-1.23 [rad/m]
Bump Steer Rear	-0.03 [rad/m]	-1.07 [rad/m]
Static Toe Angle Front	-0.05 [rad]	0.01 [rad]
Static Toe Angle Rear	-0.06 [rad]	-0.03 [rad]
Camber Suspension Front	-2.09 [rad/m]	-1.86 [rad/m]
Camber Suspension Rear	2.95 [rad/m]	0.02 [rad/m]
Camber Steer Front	-0.40 [rad/rad]	-0.05 [rad/rad]
Error	1350	1520

Table 8.12: Optimal Static Camber Angle, Bump Steer, Static Toe Angle, Camber Suspension Ratio and Camber Steer Ratio parameters for Vehsim vehicle model with measurement data from Step and Sinus driving

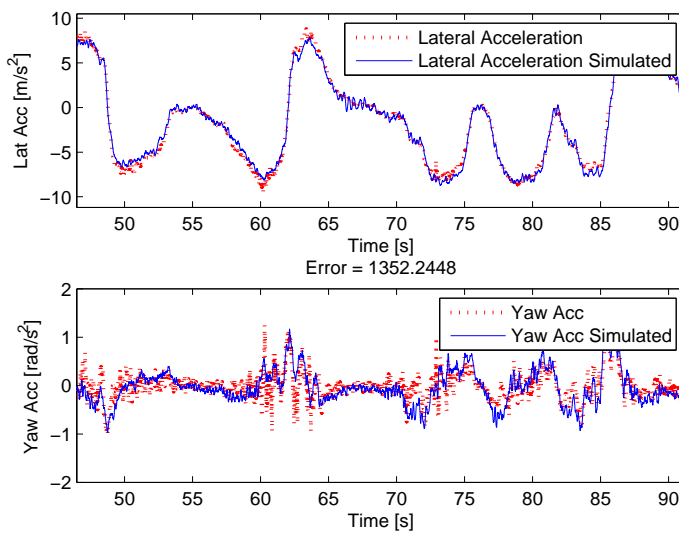


Figure 8.13: Simulation of Vehsim vehicle model with optimal values of Static Camber Angle, Bump Steer, Static Toe Angle, Camber Suspension Ratio and Camber Steer Ratio parameters and measurement data from handling track driving, high road friction.

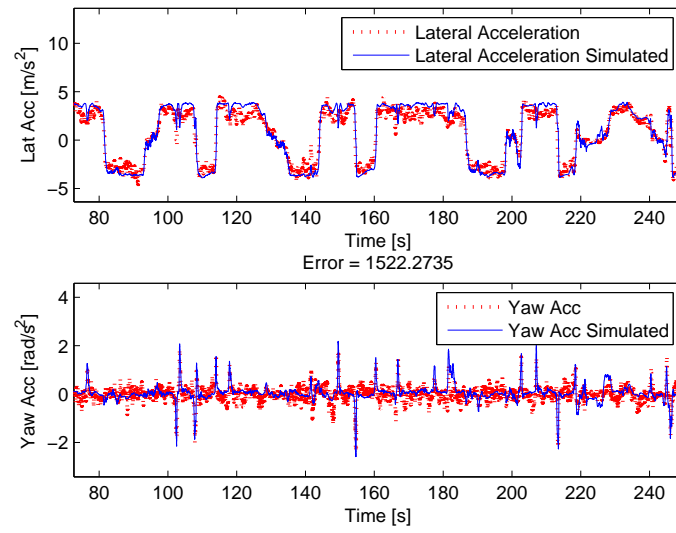


Figure 8.14: Simulation of Vehsim vehicle model with optimal values of Static Camber Angle, Bump Steer, Static Toe Angle, Camber Suspension Ratio and Camber Steer Ratio parameters and measurement data from handling track driving, low road friction.

9 | Discussion

9.1 Scaling

The lateral- and yaw acceleration measurements used for optimization of tire and chassis parameter are scaled since they are of different size. The lateral acceleration data would be considered as more important than the yaw acceleration data without scaling. During the work of writing an optimizing algorithm it turned out that how the scaling parameter is chosen substantially affect the result of the optimization.

9.2 Error

The present error function work only for comparison between high road friction vs. high road friction or low road friction vs. low road friction simulations since the error value is calculated as the norm of the difference between measured and simulated data. This means that the error value is dependent of the length of the data used and comparison is only relevant when the same measurement file is used for validation. An improvement that can be made in the optimization and simulation code is to find a better error value that can be used to compare the simulations with.

9.3 Choice of chassis parameters

The choice of which chassis parameters to optimize was done by testing different combinations of camber and toe parameters. Before the camber and toe parameters where chosen to use in the optimization, parameters concerning the suspension of vehicle was tested, for example spring and damper constants described in 4.2.3. The result of the parameter fitting with suspension parameters gave unreasonable results and it appeared as if the parameters had to compensate for events that the model could not handle. The parameter values for different optimizations gave completely different values that where unreasonable high or low. The camber and toe parameters optimization gave values that are fairly reasonable in the sense that non of the parameters values where completely wrong as in the case with the suspension parameters. The plausibility of the camber and toe parameter values that are the result of the chassis optimization can be studied further, and it is likely that some of the parameter values compensate for somethings that the model can not handle but by optimizing these parameters it is possible to get the simulation to follow measured data.

9.4 Result of bicycle model optimization

The optimized parameters in the bicycle model are the tire stiffness parameters C_{12} and C_{34} . *Figure 8.1* and *8.2* shows that the result of the optimization with data from high road friction runs shows better compliance than the low road friction data. An explanation to this is that the model does not consider friction and that the tire forces in the bicycle model are linear functions of drift angles. When driving on low friction surface the car move in the nonlinear region since all friction are used and the car slides. The linear tires in the bicycle model makes it only valid for driving on high friction or low speed where no sliding occurs.

9.5 Result of Vehsim vehicle model optimization

The optimization of Vehsim vehicle parameters are divided in radius, tire and chassis parameters optimization. The wheel radius is in fact one of the tire parameters but it is optimized separately since data for longitudinal acceleration is used, unlike the other tire parameters that are optimized with data from lateral- and yaw acceleration measurements.

Both tire and chassis parameters are optimized using lateral acceleration and yaw acceleration data and at first all parameters were optimized at the same time. It turned out that it is hard to get reasonable result of all parameters at the same time using this optimization method and that is the reason it was split in chassis and tire optimization.

9.5.1 Radius optimization

The wheel radius optimization gave wheel radius values of 0.323 m for high road friction data and 0.317 m for low road friction data which are reasonable values. *Figure 8.3* and *8.4* shows the simulated and measured data for longitudinal acceleration and it can be seen that low road friction simulation is better during the the whole run than the high road friction simulation. The important part where the car moves with constant velocity, that is when the longitudinal acceleration is around 0 m/s^2 is satisfying for both high and low road friction simulations. An improvement that can be made in the simulation code is to only use zero acceleration data for the optimizations.

9.5.2 Tire optimization

The tire scaling parameters for road friction and tire stiffness are optimized and *Table 8.4* shows the resulting parameter values. The optimization gave high road friction values of 1.06 for front wheel and 1 for rear wheel. Optimized low road friction parameters are 0.47 for front wheel and 0.43 for rear wheel. The values of the optimized friction coefficients are reasonable both for high and low road friction data since typical values of ice friction is around 0.4 and asphalt friction is around 1.

The tire stiffness scaling parameter values are optimized to 1.02 for front wheel and 2.04 for rear wheel for high road friction. The low road friction values are 0.65 for front wheel and 0.71 for rear wheels. The result shows that the rear wheels are stiffer than the front wheels both for high and low road friction measurements.

9.5.3 Chassis parameters, high road friction

The result of high road friction simulations with optimized values of chassis parameters for different parameter combinations are presented in *Chapter 8*. The case where front and rear *Static Camber Angle*, *Bump Steer*, *Static Toe Angle* and *Camber Suspension Ratio* parameters and *Camber Steer Ratio Front* are optimized give best compliance since the error value is smallest, the value is 1350 in this case. The greatest error value and therefore the least compliance between simulation and measurements for the tested combinations is received with *Static Camber Angle* and *Bump Steer Ratio* as parameters, the error value is 1500.

9.5.4 Chassis parameters, low road friction

The smallest error value for low road friction simulation with *Handling tracks* data is received when front and rear *Static Camber Angle*, *Bump Steer Ratio*, *Static Toe Angle*, *Camber Suspension Ratio* and *Camber Steer Ratio Front* parameters is optimized. The error value is 1520. The case where *Static Camber Angle* and *Bump Steer* for front and rear wheels is optimized give the highest value of the error, 2070.

9.6 Comparison between bicycle model and Vehsim vehicle model

The more complex Vehsim vehicle model works for both high and low road friction simulation while the simpler bicycle model only give good results for high road friction data. One of the main reasons is the more complex tire model used in the Vehsim vehicle model.

9.7 Optimization method

One alternative considered before the optimization algorithm was written was to use an extended Kalman filter. There is an example of how to use extended Kalman filter to fit parameters to measurement data in [3]. The reason the Kalman method not was used is that it requires an exact mathematical model which is not available this case.

10 | Conclusions

A conclusions that can be drawn after working with optimizing vehicle parameters to measurement data is that it is clearly possible to improve the behavior of the simulations both for the bicycle model and for the Vehsim vehicle model. More detailed descriptions about the conclusions for both models will follow.

10.1 Vehsim vehicle model

The work of choosing which chassis parameters to optimize for the Vehsim vehicle model was a time consuming part of this thesis. The final parameters are chosen since they change the behavior of the simulated car to the better and since the parameter values are fairly reasonable. To find an optimal set among the possible chassis parameters would require more work but a conclusion that can be drawn is that it is possible to improve the reliability in the simulations by using measurement data to optimize steering kinematics parameters. It is possible that other chassis parameters than the ones discussed in this thesis also would affect the car behavior but that can be a subject for further work.

A conclusion about the tire parameter optimization is that the resulting friction values are reasonable for both high and low road friction conditions and that the simulations with optimal tire parameters show good compliance with measurement data.

During the work of optimizing vehicle parameters it showed to be necessary to split the optimization in tire and chassis parameters instead of optimizing all parameters in one run to get reasonable values of all parameters.

10.2 Bicycle model

The bicycle model is not as complex as the Vehsim vehicle model but the results show that the model anyway can simulate the behavior of a real car, within some limitations. The case when high road friction data is used for optimization and simulation show good compliance with real measurements. The bicycle model uses simple linear expressions for the tire forces unlike the Vehsim vehicle model that uses the semi empirical Magic Tire Formula. When using low road friction data for optimization and simulation it shows that the bicycle model is not enough to simulate the behavior, partly because of the tire model.

Acknowledgement

I want to thank my supervisors at BorgWarner Pierre Pettersson, Tord Diswall and Jacco Koppenaal for their support during the work with the thesis. I want to thank my examiner at Kungliga Tekniska Högskolan, Per Enqvist.

Bibliography

- [1] H. B. Pacejka *Tyre and Vehicle Dynamics*. Butterworth-Heinemann, London Third Edition, 2012.
- [2] Anthony Bedford, Wallace Fowler *Engineering Mechanics Dynamics*. Prentice Hall, Pearson Education, Singapore, SI Edition, 2005.
- [3] Lennart Ljung, Torkel Glad *Modellbygge och simulering*. Studentlitteratur AB, Lund Upplaga 2:4, 2009.
- [4] Helsingborgs Dagblad, <http://hd.se/motor/2013/03/21/pagar-med-kansla-for-is/>
- [5] MathWorks, Matlab help documentation <http://www.mathworks.se/help/optim/ug/lsqnonlin.html>
- [6] Jacco Koppenaal, *Tyre Module Specification*, Haldex Traction AB, 2006
- [7] Erik Wennerström, *Föreläsning i fordonsdynamik*, Kungliga Tekniska Högskolan, Stockholm, 1994
- [8] Omni instruments, Motion sensor description, <http://omniinstruments.co.uk/products/product/moredetails/lpms-cu.id1479.html> 2013-07-15
- [9] S.Schoutissen, *Chassis Module Specification, Draft*, Haldex Traction AB, 2006
- [10] Pierre Pettersson, *Estimation of Vehicle Lateral Velocity*, Haldex Traction AB, 2008
- [11] Michele Russo, Riccardo Russo and Agostino Volpe (2000), *Car Parameters Identification by Handling Manoeuvres*, Vehicle System Dynamics: International Journal of Vehicle Mechanics and Mobility, 34:6, 423-436
- [12] Joga Dharma Setiawan, Mochamad Safarudin, Amrik Singh, *Modeling, Simulation and Validation of 14 DOF Full Vehicle Model*, Diponegoro University, Semarang, Indonesia and University Teknikal Malaysia Melaka, Malaysia

A | Nomenclature

α	- Lateral Slip	[rad]
α_{12}	- Drift angle front, bicycle model	[rad]
α_{34}	- Drift angle rear, bicycle model	[rad]
γ	- Velocity sensor angle	[rad]
κ	- Longitudinal Slip	[rad]
ψ	- Yaw Angle	[rad]
$\dot{\psi}$	- Yaw Rate	[rad/s]
$\ddot{\psi}$	- Yaw Acceleration	[rad/s ²]
ϕ	- Roll angle	[rad]
θ	- Pitch Angle	[rad]
ϕ_{camber}	- Camber angle	[rad]
θ_{caster}	- Caster Angle	[rad]
ψ_{toe}	- Toe Angle	[rad]
δ	- Steering Wheel angle	[rad]
$\bar{\omega}$	- Rotation of body coordinate system	[rad/s]
ω_x	- Rotation around x-axis	[rad/s]
ω_y	- Rotation around y-axis	[rad/s]
ω_z	- Rotation around z-axis	[rad/s]
ρ	- Air density	[kg/m ³]
A	- Front area	[m ²]
a	- Lateral distance from center of gravity to velocity sensor	[m]
\bar{a}	- Acceleration	[m/s ²]
a_x	- Longitudinal acceleration	[m/s ²]
a_y	- Lateral acceleration	[m/s ²]
a_y, sensor	- Sensor value of lateral acceleration	[m/s ²]
b	- Longitudinal distance from center of gravity to velocity sensor	[m]
B	- Stiffness factor in magic tire formula	[—]
C	- Shape factor in magic tire formula	[—]
C_{12}	- Tire constant front wheel, bicycle model	[N/rad]
C_{34}	- Tire constant rear wheel, bicycle model	[N/rad]
C_D	- Drag coefficient	[—]
$c_{antirollbar}$	- Spring coefficient anti roll bar	[N/m]
c_{damper}	- Damper constant	[Ns/m]

c_{spring}	- Spring constant	[N/m]
D	- Peak factor in magic tire formula	[−]
E	- Curvature factor in magic tire formula	[−]
\hat{e}_x	- Unit vector x-direction	[−]
\hat{e}_y	- Unit vector y-direction	[−]
\hat{e}_z	- Unit vector z-direction	[−]
F_{12}	- Tire force front wheel, bicycle model	[N]
F_{34}	- Tire force rear wheel, bicycle model	[N]
F_x	- Longitudinal force	[N]
F_y	- Lateral force	[N]
F_{drag}	- Aerodynamic drag force	[N]
\bar{F}_{fl}	- Tire force, front left wheel	[N]
\bar{F}_{fr}	- Tire force, front right wheel	[N]
\bar{F}_{rl}	- Tire force, rear left wheel	[N]
\bar{F}_{rr}	- Tire force, rear right wheel	[N]
F_t	- Tire force, spring damper system	[N]
F_{damper}	- Damper force, spring damper system	[N]
F_{spring}	- Spring force, spring damper system	[N]
g	- Gravity constant	[m/s ²]
I_{xx}	- Moment of inertia around x-axis	[kg · m ²]
I_{yy}	- Moment of inertia around y-axis	[kg · m ²]
I_{zz}	- Moment of inertia around z-axis	[kg · m ²]
l_f	- Distance from CoG to front wheel in bicycle model	[m]
l_r	- Distance from CoG to rear wheel in bicycle model	[m]
m	- Mass of vehicle body	[kg]
m_{hub}	- Mass of wheel	[kg]
m_i	- Mass of i:th particle	[kg]
\bar{r}	- Position vector of center of gravity, bicycle model	[m]
$\dot{\bar{r}}$	- Velocity vector of center of gravity, bicycle model	[m/s]
R_ϕ	- Rotation matrix, roll	[−]
R_θ	- Rotation matrix, pitch	[−]
R_ψ	- Rotation matrix, yaw	[−]
\bar{R}_i	- Position vector from center of gravity to i:th particle	[m]
$\dot{\bar{r}}_f$	- Velocity vector of front wheel, bicycle model	[m/s]
$\dot{\bar{r}}_r$	- Velocity vector of rear wheel, bicycle model	[m/s]
r_{fl}	- Position of front left wheel in body coordinate system	[m]
r_{fr}	- Position of front right wheel in body coordinate system	[m]
r_{rl}	- Position of rear left wheel in body coordinate system	[m]
r_{rr}	- Position of rear right wheel in body coordinate system	[m]
T	- Transformation matrix, local to global	[−]
V	- Velocity	[m/s]
v_x	- Velocity x-direction	[m/s]
v_y	- Velocity y-direction	[m/s]

v_z	- Velocity z-direction	$[m/s]$
v_{sensor}	- Velocity sensor value	$[m/s]$
z_{hub}	- Position of wheel hub	$[m]$
\dot{z}_{hub}	- Velocity of wheel hub	$[m/s]$
\ddot{z}_{hub}	- Acceleration of wheel hub	$[m/s^2]$

B | Vehsim signals

B.1 Chassis

<i>Input from</i>	<i>Input signals</i>	<i>Output signals</i>
Driver	SteeringWheelAngle	GlobalVelocity
Tire	GlobalTireForces	GlobalPosition
		EulerAngles
		Global2bodyDCM
		Global2bodyDCMdot
		BodyVelocity
		BodyAcceleration
		pqr
		$\dot{p}\dot{q}\dot{r}$
		GlobalHubPosition
		GlobalHubVelocity
		Global2HubDCM
		SteerAngleMean

Table B.1: Chassis inputs and outputs

B.2 Tire

<i>Input from</i>	<i>Input signals</i>	<i>Output signals</i>
Chassis	Global2HubDCM	GlobalTireForce
	GlobalHubVelocity	HubTireForce
Road	RoadNormal	WheelOmega
	HubtoRoad Distance	TireTrq
PowerTrain	RoadFriction	Deqvar
	HubTrq	
	HubBrakeTrq	

Table B.2: Tire inputs and outputs

B.3 Power train

<i>Input from</i>	<i>Input signals</i>	<i>Output signals</i>
Driver	BrakePedal	HubBrakeTrq
	HandBrake	HubTrq
	ThrottlePedal	CEngOmega
	ClutchPedal	CEngTrq
	SelectedGear	FootClutch DiffOmega
	ReqCengTrq	HLSCL DiffOmega
Tire	WheelOmega	XWD DiffOmega
	FXD PressSP	FXD DiffOmega
Control software	HLSCL PressSP	
	XWD PressSP	
	ABS BrakeTrqLim	

Table B.3: Power train inputs and outputs

B.4 Fuel consumption

<i>Input from</i>	<i>Input signals</i>	<i>Output signals</i>
Power train	CEngOmega	FuelConsumptionRate
	CEngTrq	FuelConsumed

Table B.4: Fuel consumption inputs and outputs

B.5 Driver

<i>Input from</i>	<i>Input signal</i>	<i>Output signal</i>
Road	RoadUV	Steering wheel angle
	Road Yaw Direction	Throttle Pedal
	RoadVFuture	Brake Pedal
Vehicle	Global Position	Clutch Pedal
Vehicle	Euler angles	Selected gear
	pqr	Hand brake
	Body Velocity	Requested Combustion engine torque
	Foot clutch diff omega	
	Combustion engine omega	
Vehicle	Wheel Omega	

Table B.5: Driver model inputs and outputs

B.6 Road

<i>Input from</i>	<i>Input signal</i>	<i>Output signal</i>
Vehicle model	Global Hub Position	Road Yaw Direction
	Global Position	RoadUV
	Global Velocity	Road V Future
		RoadV Future 2
		Hub to road Distance
		Road Normal
		Road Friction

Table B.6: Road model inputs and outputs

TRITA-MAT-E 2013:42
ISRN-KTH/MAT/E—13/42-SE